# SOLID ADSORPTION MEDIA FOR HF & HCl FOLLOWING REFRIGERANT DESTRUCTION

by

Tekai Akuetteh

Submitted in partial fulfillment of the requirements for the degree of

Master of Applied Science

at

Dalhousie University

Halifax, Nova Scotia

August 2013

## TABLE OF CONTENTS

## LIST OF TABLES

## LIST OF FIGURES

## ABSTRACT

This work explored the viability of two solid adsorbents, limestone and cement powder, for use in a flow-through packed-bed column for HCl and HF gas neutralization following refrigerant destruction. Neutralization tests performed at 408 K using 5% HCl in $N_2$ and 5% HF in $N_2$, showed that limestone had a significantly higher adsorption capacity for both HF & HCl, future tests therefore utilized limestone only. The results showed that ~49% of the fed HCl and between 7.8% - 16.2% of the fed HF gases were adsorbed by 0.007 kg of limestone for a $6.67\times10^{-6}$ $m^3/s$ (STP) flow rate over 30 – 180 minutes. Applying the shrinking core model, effective diffusivities ($D_e$) of HCl & HF into the limestone particles were $1.5\times10^{-9}$ & $2.2\times10^{-9}$ $m^2/s$ respectively. Under these conditions, complete particle conversion times were 227 hours for HCl–limestone and 154 hours for HF–limestone. Estimating $D_e$ values at plasma-reactor temperatures gave $5.61x10^{-9}$ $m^2/s$ & $8.24x10^{-9}$ $m^2/s$ for HCl–limestone and HF–limestone respectively. Correspondingly, particle consumption times were reduced to 61 and 41 hours for HCl–limestone and HF–limestone. Considering the conversion times for the 1 mm particle sizes, shorter conversion times would require micron-scale particle sizes, suitable for entrained flow but not for a packed-bed arrangement.

## LIST OF ABBREVIATIONS AND SYMBOLS USED

ABBREVIATIONS

| | |
|---|---|
| avg | Average |
| $CCl_2F_2$ | CFC-12 |
| CFC | Chlorofluorocarbons |
| CFO | Critical Flow Orifice |
| HCFC | Hydrochlorofluorocarbons |
| HCl | Hydrochloric acid |
| HF | Hydrofluoric acid |
| ISE | Ion Selective Electrode |
| MD | mini-DIN pin |
| $N_2$ | Nitrogen gas |
| ORP | Oxidation-Reduction Potential |
| SCM | Shrinking Core Model |
| STP | Standard Temperature & Pressure (293 K, 101.3 kPa) |
| UV | Ultra-violet |

SYMBOLS

| | |
|---|---|
| $b$ | Stoichiometric coefficient of solid in chemical reaction |
| $C_A$ | Concentration of gas ($mol/m^3$) |
| $C_{Ac}$ | Concentration of gas at unreacted core ($mol/m^3$) |

| | |
|---|---|
| $C_{As}$ | Bulk phase concentration of gas at particle surface (mol/m$^3$) |
| $C_v$ | Coefficient of flow |
| $d_p$ | Particle diameter (m) |
| $D_{AB}$ | Diffusion coefficient of gaseous mixture (HCl-Nitrogen, HF- Nitrogen) (m$^2$/s) |
| $D_e$ | Effective diffusivity (m$^2$/s) |
| $k$ | Boltzmann constant |
| $L$ | Bed length (m) |
| $m$ | Mass (kg) |
| $M_A$ | Molecular mass of HCl (g/mol) |
| $M_B$ | Molecular mass of HF (g/mol) |
| $N_A$ | Moles of gas (moles) |
| $P$ | Pressure (Pa) |
| $\Delta P$ | Change in pressure (Pa) |
| $Q_A$ | Molar flux |
| $Q_{Ac}$ | Molar flux at unreacted core |
| $Q_{As}$ | Molar flux at particle surface |
| $Q_G$ | Gas flow rate in CFO (m$^3$/s) |
| $r$ | Radius of particle at any time $t$ (mm) |
| $r_c$ | Radius of unreacted core (mm) |
| $R$ | Initial radius of particle (mm) |

| | |
|---|---|
| $t$ | Time (sec) |
| $t_c$ | Time for complete particle consumption (sec) |
| $T$ | Temperature (K) |
| $T_b$ | Normal boiling point temperature (K) |
| $u_0$ | Superficial fluid velocity (m/s) |
| $V_b$ | Liquid molar volume at normal boiling point ($cm^3$/mol) |
| wt% | Weight percentage |
| $X$ | Conversion |
| $y$ | Volume fraction of calcium carbonate remaining in solid after exposure to HF gas |

GREEK LETTERS

| | |
|---|---|
| $\varepsilon$ | Bed void fraction |
| $\mu_p$ | Dipole moment (Debye) |
| $\mu$ | Fluid dynamic viscosity (Pa·s) |
| $\rho$ | Fluid density ($kg/m^3$) |
| $\rho_B$ | Molar density of $CaCO_3$ ($mol/m^3$) |
| $\sigma_A$ | Lennard-Jones length for HCl or HF (Å) |
| $\sigma_B$ | Lennard-Jones length for Nitrogen (Å) |
| $\sigma_{AB}$ | Characteristic length for HCl-Nitrogen or HF-Nitrogen (Å) |
| $\sigma_c$ | Constriction factor |
| $\tau$ | Tortuosity |

| | |
|---|---|
| $\phi_c$ | Volume fraction of $CaCO_3$ in solid particle |
| $\phi_p$ | Particle porosity |
| $\Omega_D$ | Dimensionless diffusion collision integral |

## ACKNOWLEDGEMENTS

I would like to first and foremost thank God Almighty for my life and for the great people He has blessed me with who made this study a success. I am extremely grateful to my dad, sisters, Henry and all my family, whose financial provision, emotional support and silent encouragement have made it possible for this work to come to a completion. I love you all so much and this would not have been possible without you in my life.

My heartfelt gratitude also goes to my supervisory team, Dr. Michael Pegg, Dr. Stephen Kuzak, Dr. Mark Gibson and especially Dr. Adam Donaldson, who was extremely patient with my shortfalls and came to my aid throughout the entire duration of this project. I pray that God blesses you and your family abundantly, and when you need it, may there always be someone ready to help you, just like you did for me. Also to NSERC, for financially supporting me during the course of this work.

My sincerest thanks also goes to Mr. Ray Dube, whose help during the experiments contributed to the success of this work and also to Mr. Jesse Keane for his assistance.

To all my friends whom I call my 'Halifax Family'; who gave me a break from academics when I needed to rejuvenate, prayed with me, encouraged me when I needed it and gave me a social life apart from school, a great thank you to you all, this work would not have been a success without you wonderful people. Especially to Afram, taking my first two classes with you made it so much easier to adjust and this work is the culmination of those adjustments; God bless you so much.

Finally to those whose names I haven't mentioned here, you are greatly appreciated for your contributions to the success of this work. I am extremely blessed and grateful to have had you in my life during this phase of my life and I pray for God's greatest blessings for you and your loved ones, now and always.

# 1. INTRODUCTION

## 1.1. SYNOPSIS

Microwave plasma technology has recently been considered as a destruction method for waste refrigerants phased out by the Montreal Protocol. This process results in the generation of the off–gases carbon dioxide, hydrochloric (HCl) and hydrofluoric (HF) acids. This work explores the viability of two solid adsorbents, limestone and cement powder, for use in a flow-through packed–bed column used to neutralize the products of refrigerant destruction. Basic neutralization tests were performed at 408 K using 5% HCl in $N_2$ and 5% HF in $N_2$ passed through a heated tubular reactor containing the adsorption media. Of the two adsorbents tested, limestone demonstrated a significantly higher adsorption capacity for both HF and HCl, and therefore subsequent tests utilized limestone only. The results obtained showed that approximately 49% of the fed HCl and between 7.8% – 16.2% of the fed HF gases were adsorbed by 0.007 kilograms of limestone for a flow rate of $6.67\times10^{-6}$ $m^3/s$ (STP) over 30 to 180 minutes. Applying the shrinking core model, the effective diffusivities ($D_e$) of HCl and HF into the limestone particles were $1.5\times10^{-9}$ and $2.2\times10^{-9}$ $m^2/s$, respectively. Under these conditions, complete particle consumption would require 227 hours for the HCl runs and 154 hours for the HF runs. The effective diffusivity at plasma–reactor temperatures was estimated to be $5.61\text{x}10^{-9}$ $m^2/s$ for HCl into limestone and $8.24\text{x}10^{-9}$ $m^2/s$ for HF into limestone HF into limestone respectively. Correspondingly, particle consumption times were reduced to 61 hours for HCl-limestone and 41 hours for HF-limestone. Comparing the $D_e$ values calculated theoretically to the bulk diffusivity of the gases, a consistent ratio of 0.005% was found for both the HCl and HF gases, which suggested that there was a linear correction factor based on the internal properties of the solid particles. Considering the conversion times estimated for the 1 mm particle sizes, shorter conversion times (i.e. on the order of minutes) would require micron-scale particle sizes, suitable for entrained flow but not for a packed-bed arrangement. Furthermore, the slurry–based neutralization solutions were observed to efficiently neutralize the effluent gases exiting the reactor and it is therefore recommended that a liquid–based adsorption system be considered for the neutralization of the acidic gases generated from waste refrigerant destruction using a plasma reactor.

## 1.2. BACKGROUND INFORMATION

The phase-out of ozone-depleting refrigerants such as chlorofluorocarbons (CFCs) and hydrochlorofluorocarbons (HCFCs) since the Montreal Protocol was agreed on by the signatory nations in 1987, has led to an accumulation of these ozone depleting substances which need to be destroyed.[1] Identified technologies for the destruction of these halocarbons include thermal processes, chemical processes and electrical processes.[2] These include cement kilns, rotary kiln incineration, liquid injection incineration, gaseous oxidation, nitrogen plasma arc, microwave plasma and argon plasma arc to name but a few.[3]

Thermal processes use heat to decompose the halocarbons and these consist of thermal incineration where high temperatures and excess oxygen are needed for the destruction; catalytic incineration where the presence of a catalyst speeds up the break down process and therefore relatively lower temperatures are used; and pyrolysis where high temperatures destroy the halocarbons in the absence of oxygen.[2] These processes are the most widely used in halocarbon break down.[4-6]

Chemical processes use chemicals to aid with the destruction process. These include active metal scrubbing where active metals react with the halocarbons to result in their destruction, chemical scrubbing where highly alkaline non-aqueous liquor absorbs the halocarbons, wet air oxidation which involves the use of a moderate temperature aqueous stream to break down the halocarbons mainly by hydrolysis, and supercritical water oxidation[7] which is similar to wet air oxidation but occurs at higher temperatures and pressures to increase the reaction rate.[2]

Electrical processes use high voltages to generate energized electrons, capable of destroying waste materials.[2] Plasma technologies have been used in different industries over the years. In recent times, research into their application in waste treatment processes has led to their consideration for CFC and HCFC destruction. This is because they have a wide range of advantages which include the use of electricity as their power source which results in more process chemistry options, control of the process environment, lower off-gas flow rates and thus lower gas cleaning costs and the

possibility of producing marketable co-products; their high energy densities and temperatures which permit rapid heating and reactor startup, high heat and reactant transfer rates, smaller installation sizes and high quench rates.[8,9] Thermal, argon, nitrogen arc and microwave plasma technologies have been used by different researchers to break down halocarbons.[3,8,10] The most widely used system is the PLASCON argon arc process.[3,8,11]

The plasma process is preferred to the incinerator processes because the waste halocarbons are usually in concentrated form, and therefore the energy provided during the process goes solely into breaking down the wastes. However, due to the high chlorine and fluorine content of CFCs and HCFs, the plasma process seems unattractive because of the generation of corrosive by-products which may result in significant equipment damage, as well as health and safety risks.[12]

The microwave plasma technology has been considered by the industry partner involved with this study for the destruction of waste refrigerants. It has proven to be efficient in destroying the waste CFCs and HCFCs however; it results in the generation of hydrochloric and hydrofluoric acid by–products.[13] Considering the hazardous nature of these acids, they cannot be released directly into the environment. A process to neutralize them is therefore necessary in order for the destruction procedure of the halocarbons to be complete. The process of neutralizing the by-product acids may be a wet or dry process.

Flue gas treatments use wet or dry scrubbers to clean the waste gases generated by the industrial processes.[14,15] Wet scrubbers have been used over the years in flue gas treatment units to treat sulfur dioxide and other acidic gases. They are described as wet scrubbers because they employ liquids to clean the waste gases that are generated in the systems in which they function. The liquids used in such systems may vary from alcohols to amines;[14] however the most common liquid is water. This serves as a base solution into which an appropriate chemical, commonly sodium hydroxide or potassium hydroxide, may be dissolved in order to neutralize the by-product acidic gases that are generated. However, wet scrubbers are not always the preferred systems for neutralizing waste acidic gases. When choosing between a wet or dry scrubber, the factors to consider include the nature of the process that generates the gases, the required properties of the

absorber vessel, the necessary equipment, the energy and pumping requirements and waste handling.[15] Dry scrubbers use alkaline solid materials to neutralize the waste acidic gases generated by processes. However, with solid waste handling, the relatively lower amounts of the neutralization materials that is used results in the use of comparatively larger volumes of solids thereby generating large volumes of waste generated.[15] When compared to the wet scrubber process, these make the choice of a dry scrubber seem unfavorable.

The ideal acidic gas treatment system should be able to react completely with the acidic gases at the conditions under which they are produced. Such conditions are usually temperatures around 873 K and medium to high gas flow rates. The time needed for complete reaction, the method for exposing the gases to the adsorbent and the cost of running the process will also have to be taken into consideration when deciding what acidic gas treatment system is ideal.

For this study, a dry scrubber system was preferred mainly because the waste materials after the neutralization process would be much easier to handle. Furthermore, considering the design of the system to mimic the high temperatures at which the acidic gases are generated, it would be much easier and convenient if a dry scrubber reactor unit was used. In addition, a similar process was utilized by Yasui et al [16] as they studied gas solid reactions between solid adsorbents and fluorine gases.

To carry out a successful neutralization process similar to a dry scrubber system, a solid material, preferably alkaline in nature was used. A reactor unit was packed with a known mass of the solid material and heated up in an electric furnace. Because of the cost of a microwave plasma unit, the acidic gases were simulated using HCl and HF supplied from cylinders, which was fed directly to the reactor unit instead of being by-products from the decomposition of halocarbons.

The search for a suitable adsorbent led to a study on chemical products that are produced from reactions directly involving HCl or HF with some other material. This is because the adsorbent to be used will eventually be reacting directly with these acids, and therefore in the search for an adsorbent, it's best to find materials that will readily react

with the acidic gases to produce a chemically stable finished product. Depending on the quality of the finished by-products from the neutralization process, there is the potential for them to be sold to other industries as raw materials, would provide additional economic benefit. This, however, depends largely on the choice of solid adsorbent used. Detailed analysis and the criteria for choosing potential adsorbents are found in Chapter 3.

The objective of this investigation is to:

- Study the feasibility of solid media for the neutralization of HF and HCl gases generated from refrigerant break down.

Limestone was chosen as the preferred solid adsorbent from the various options discussed and it was incorporated into the experimental system as a bed of particles within a reactor where it was exposed to the flow of the acidic gases. A description of the analysis methodology (the Shrinking Core Model (SCM)) used to interpret the results obtained from the experimental system is also outlined in Chapter 2. Details of the key components of the lab setup used to neutralize the HCl and HF gases at high temperatures and the operation of the system are found in Chapter 4. The SCM is used to estimate the effective diffusivity of the acidic gases into the limestone particles. An approximate time for complete particle reaction within the system was thereby estimated, with the results discussed within the context of the refrigerant destruction application in Chapter 5. Chapter 6 outlines the inadequacies observed from the investigation and thus recommends future work possibilities. Calibration data and other relevant information which could not be included in the main body of the report are found in the Appendices.

# 2. THEORETICAL BACKGROUND ON THE ANALYSIS OF GAS – SOLID REACTIONS

## 2.1. INTRODUCTION TO GAS ADSORPTION ON SOLIDS

Adsorption reactions between solids and gases occur via three mechanisms, namely chemical reactions between the gas and the solid, external gas diffusion and internal gas diffusion. Internal diffusion for porous solids may occur through pore and/or solid diffusion. Depending on the nature of the solids and the reactions taking place, one or both of these internal mechanisms may be controlling. Fig 2.1. shows a simple illustration of the diffusion mechanisms as may be occurring between gaseous molecules and a solid particle.

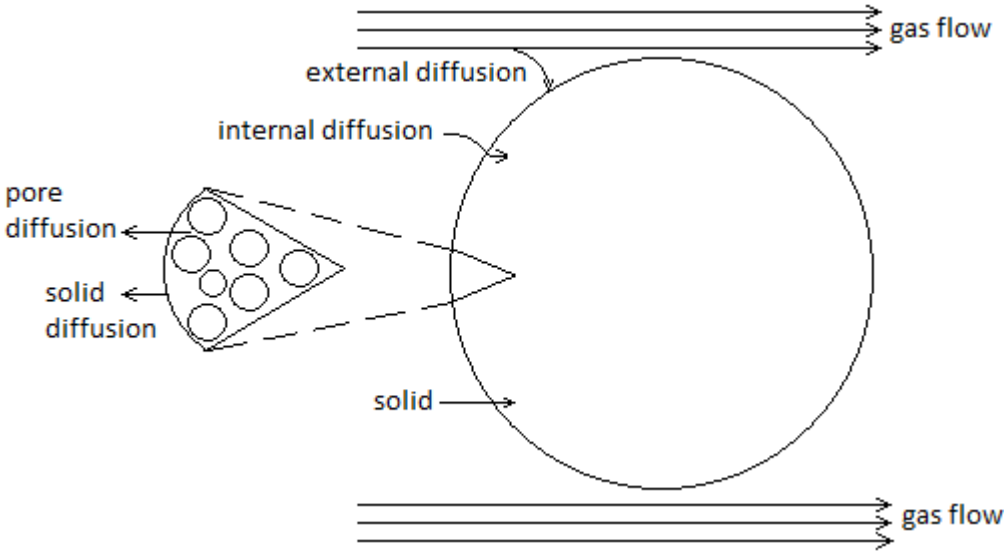


**Figure 2.1.** Diagram showing the different diffusion mechanisms for reactions between solid particles and gaseous molecules.

For systems where internal diffusion dominates the rate at which the adsorption process occurs, it is assumed that the rate of the chemical reaction is reasonably fast and external diffusion is negligible. The shrinking core model (SCM) has been applied by several researchers to the study of gas-solid reactions over a wide range of applications.
17-25

## 2.2. THE SHRINKING CORE MODEL (SCM)

The model is based on the principles that the gaseous molecules diffuse through the bulk gas film to the external solid surface, these molecules penetrate and diffuse through the 'ash' layer (The term 'ash' refers to the completely reacted, inert solid layer formed on the outer core of the solid particle which is porous enough to allow gases to penetrate it into the unreacted core.[27,28]) to the unreacted core surface, the gases react with the solids at the unreacted core surface, the products from the reaction diffuse through the formed 'ash' layer to the external solid surface and finally the gaseous products diffuse through the gas film back into the bulk gas stream.[26] The factors that most influence the rate of a porous particle reaction are the surface reaction and pore diffusion.[27] Therefore, for this investigation the reaction between the acidic gases and the limestone particles and all the other steps mentioned in this paragraph were assumed to be fast, except for the diffusion of the gases into the particle. Taking these into account, the derivation of a suitable equation to represent the reaction between spherical limestone particles and HCl/HF gases will be discussed as follows. The chemical equation for the reaction between calcium carbonate and hydrochloric acid/hydrofluoric is:

$$2HCl_{(g)} + CaCO_{3(s)} \longrightarrow CaCl_{2(s)} + CO_{2(g)} + H_2O_{(g)} \quad (2.1)$$

$$2HF_{(g)} + CaCO_{3(s)} \longrightarrow CaF_{2(s)} + CO_{2(g)} + H_2O_{(g)} \quad (2.2)$$

A pseudo-steady state assumption was made, i.e. the concentration of the gas in the 'ash' layer was deemed to be constant. For a gas solid system, this means that the flow rate of the gas to the unreacted core surface is relatively faster than the size reduction of the unreacted core.[27] The reaction rate of the gas at any instant is therefore given by [27,28]:

$$-2\frac{dN_A}{dt} = 4\pi r^2 Q_A = 4\pi R^2 Q_{As} = 4\pi r_c^2 Q_{Ac} = \text{constant} \quad (2.3)$$

The flux $Q_A$ is expressed using Fick's law of equimolar counter diffusion:

$$Q_A = D_e \frac{dC_A}{dt} \quad (2.4)$$

Where $D_e$ is the effective diffusivity of the acidic gas within the 'ash' layer of the limestone particles. This value is unique to every solid material based on its pore structure and operation conditions, and therefore for this study it is the value of interest.

Combining eqns. 2.3 and 2.4 for any radius *r*,

$$-\frac{dN_A}{dt} = 4\pi r^2 D_e \frac{dC_A}{dr} = \text{constant} \tag{2.5}$$

Integrating across the 'ash' layer from *R* to $r_c$,

$$-\frac{dN_A}{dt}\int_R^{r_c}\frac{dr}{r^2} = 4\pi D_e \int_{C_{Ag}=C_{As}}^{C_{Ac}=0} dC_A \tag{2.6}$$

$$-\frac{dN_A}{dt}\left(\frac{1}{r_c}-\frac{1}{R}\right) = 4\pi D_e C_{As} \tag{2.7}$$

Eliminating $N_A$ by writing it in terms of $r_c$ and integrating eqn. 2.7 with respect to time and radius,

$$-\rho_B \int_{r_c=R}^{r_c}\left(\frac{1}{r_c}-\frac{1}{R}\right) r_c^2 dr_c = bD_e C_{As}\int_0^t dt \tag{2.8}$$

$$t = \frac{\rho_B R^2 \phi_C}{6bD_e C_{As}}\left[1-3\left(\frac{r_c}{R}\right)^2+2\left(\frac{r_c}{R}\right)^3\right] \tag{2.9}$$

Where $\rho_B$ [mol/m$^3$ particle] is the molar density of the reacting species (the solid $CaCO_3$), $\phi_C$ is the volume fraction of solid material, *b* is the stoichiometric coefficient of the solid in the chemical reaction, $C_{As}$ is the bulk phase concentration of HCl or HF, and $r_c$ and *R* are the unreacted front position and outer radius of the particle, respectively whose values are estimated from the volume of particle reacted via the measured chloride/fluoride ion content of the solids.

For complete particle reaction, $r_c$ = 0 and therefore, the time for complete reaction becomes

$$t_c = \frac{2\rho_B R^2 \phi_C}{6bD_e C_{As}} \tag{2.10}$$

The effective diffusivity values were estimated using the experimental results obtained from the runs and eqns. 2.9 and 2.10.

To compare the rate of particle conversion with respect to time, eqn. 2.9 was divided by eqn. 2.10 to obtain

$$\frac{t}{t_c} = \left[1 - 3\left(\frac{r_c}{R}\right)^2 + 2\left(\frac{r_c}{R}\right)^3\right] \tag{2.11}$$

But 1 – X = fraction of unreacted solid = $\frac{core\ volume}{particle\ volume} = \frac{\frac{4}{3}\pi r_c^3}{\frac{4}{3}\pi R^3} = \left(\frac{r_c}{R}\right)^3$

Therefore $\frac{r_c}{R} = (1 - X)^{1/3}$ where X refers to conversion.

Writing eqn. 2.11 in terms of conversion,

$$t = \left[1 - 3(1 - X)^{2/3} + 2(1 - X)\right] t_c \tag{2.12}$$

For the experimental conversion values obtained, the time *t* that it would take to attain these conversions were calculated. The values of the time and corresponding conversion were then plotted as the predicted conversion estimates under the experimental conditions for the HCl and HF runs.

From eqn. 2.12, it can be seen that the time for complete particle conversion is directly proportional to the time it takes to reach a definite conversion. Indirectly though, this $t_c$ value is influenced by the effective diffusivity values (see eqn. 2.10; which varies under the experimental and higher plasma reactor temperatures) and therefore the estimated rate of conversion with respect to time under the plasma reactor conditions does vary from those at the experimental conditions as will be seen in Section 5.3.2.

## 2.3. THEORETICAL EFFECTIVE DIFFUSIVITY ESTIMATIONS

The theoretical effective diffusivity of the acidic gases within the limestone particles under the experimental conditions were calculated using eqn. 2.13. This equation shows that there is a linear correlation between the bulk diffusivity ($D_{AB}$) and effective diffusivity ($D_e$) which is dependent on the pore properties of the particles.

$$D_e = \frac{D_{AB}\phi_p\sigma_c}{\tau} \tag{2.13}$$

Where $D_{AB}$ is the diffusion coefficient of the gaseous mixture in $cm^2/s$, $\phi_p$ is the particle porosity assumed to be 0.4, $\sigma_c$ is the constriction factor assumed to be 0.8 and $\tau$ is the tortuosity assumed to have a value of 3.0.[29] These values reflect assumed properties typical to pore-diffusion limited mass transfer in solid particles. The diffusion coefficient ($D_{AB}$) of a binary gaseous mixture may be found using the modified Chapman-Enskog equation (eqn. 2.14).[30]

$$D_{AB} = \frac{0.00266T^{3/2}}{PM_{AB}^{1/2}\sigma_{AB}^2\Omega_D} \tag{2.14}$$

Where $T$ is the temperature in Kelvin, $P$ is the pressure in bar,

$M_{AB} = 2\left(\frac{1}{M_A} + \frac{1}{M_B}\right)^{-1}$ $M_A$ and $M_B$ are the molecular weights of HCl/HF and nitrogen gas respectively,

$\sigma_{AB} = (\sigma_A\sigma_B)^{1/2}$ $\sigma_A$ and $\sigma_B$ is the Lennard-Jones length in Angstrom (Å) for HCl/HF and nitrogen respectively,

$$\Omega_D = \frac{1.06036}{T^{*0.15610}} + \frac{0.19300}{\exp(0.47635T^*)} + \frac{1.03587}{\exp(1.52996T^*)} + \frac{1.76474}{\exp(3.89411T^*)}$$

$$T^* = \frac{kT}{\varepsilon_{AB}} \text{ and } \frac{\varepsilon_{AB}}{k} = \left(\frac{\varepsilon_A}{k} \times \frac{\varepsilon_B}{k}\right)^{1/2}$$

The values for $\varepsilon_A/k$ and $\varepsilon_B/k$ are obtained from the Lennard-Jones potentials for HCl/HF and nitrogen.[30]

For polar gases like HF and HCl, $\Omega_D^* = \Omega_D + \frac{0.19\delta_{AB}^2}{T^*}$

$\delta_{AB} = (\delta_A \delta_B)^{1/2}$ and $\delta = \frac{1.94 \times 10^3 \mu_p^2}{V_b T_b}$, where $\mu_p$ is the dipole moment in Debyes, $V_b$ is the liquid molar volume at normal boiling point in $cm^3/mol$ and $T_b$ is the normal boiling point temperature at 1 atm in Kelvin.

The values for the above mentioned parameters are available in Table 2.1.[30]

**Table 2.1.** Parameter Values Used to Calculate Diffusion Coefficients of HCl and HF in Nitrogen.[30]

| **Compound** | **Molecular weight g/mol** | **$\sigma$, Å** | **$\varepsilon/k$, K** | **Dipole moment $\mu_p$, Debye** | **$T_b$ K** | **$V_b$ $cm^3/mol$** |
|---|---|---|---|---|---|---|
| **$N_2$** | 28.014 | 3.798 | 71.4 | 0.0 | 77.35 | 34.84 |
| **HCl** | 36.461 | 3.339 | 344.7 | 1.1 | 188.15 | 30.28 |
| **HF** | 20.006 | 3.148 | 330 | 1.8 | 292.68 | 20.69 |

Using eqns. 2.13 and 2.14, together with the values provided in Table 2.1., the effective diffusivities ($D_e$) and the time for complete particle reactions for the two gaseous mixtures in limestone were estimated and the values summarized in Table 2.2. (see Appendix A1. for detailed calculation).

**Table 2.2.** Summarized Table Showing the Theoretical $D_e$ and Expected Time for Complete Reaction of Limestone Particles

| Gas | $D_{AB}$ ($m^2/s$) | $D_e$ ($m^2/s$) | Particle size range (mm) | Time (sec) |
|---|---|---|---|---|
| | | | $0.625 < R < 1.18$ | 822.57 |
| **HCl** | $3.11\times10^{-5}$ | $3.13\times10^{-6}$ | $0.584 < R < 0.625$ | 369.04 |
| | | | $0.298 < R < 0.584$ | 196.18 |
| **HF** | $3.86\times10^{-5}$ | $4.12\times10^{-6}$ | $0.584 < R < 0.625$ | 296.76 |

The rate of reaction may be done either by measuring tracking changes in the particle properties using gravimetry, visual examination [31] or chemical analysis of the reacted pellets [32] or by measuring changes in the downstream gas properties by analyzing the gas stream for gaseous reaction products using infrared absorption, water vapour condensation or absorption, gas chromatography.[33] For this study, the chloride and fluoride content of the reacted limestone solids from the reactor were measured to show how much of the acidic gases HCl and HF reacted with the solids.

# 3. ADSORBENT SELECTION

The breakdown of a stream of CFCs and HCFCs produces gaseous hydrogen chloride (HCl) and hydrogen fluoride (HF) at about 873 K. The acidic gases produced cannot be directly released into the environment and must be neutralized. To determine an approximate rate of adsorbent consumption, the expected HF and HCl generation rate for a 12,000 kg/month refrigerant destruction rate was determined. For simplicity, CFC-12 ($CCl_2F_2$) was used in the analysis. Based on this refrigerant composition, the destruction of 12,000 kg of waste $CCl_2F_2$ would produce approximately 7230 kg of HCl and 3970 kg of HF each month.

A suitable system to neutralize these gases must contain an alkali material, that is stable at fairly high temperatures and whose final products after reacting are also stable at these high temperatures. The preferred adsorbent should be able to react with both gases and produce stable products from each reaction. The ease of separation of a mixed product will be an added advantage. Furthermore, the source of the adsorbent should be close by and affordable.

Some readily available raw materials that can be used as adsorbents include alumina, soda ash, caustic soda, magnesium sulfate, calcium carbonate and ordinary Portland cement. The products from the reaction of these materials with the acids in industry and laboratories are marketable and have been found to serve as raw materials or intermediates in several industries. Also, the market for the finished products has been found to mostly be in Canada and the USA. This means that if these products meet the required standards, and are produced in reasonable quantities, they will most likely have a ready market.

The preference is to end up with some material that can be safely reused by other industries and if it brings in some profit, that will be appreciated. At the very least, in the end, a product that can be disposed of in a benign way is a reasonable target.

The objective of this Chapter is to study the potential adsorbents by providing some information on the expected finished products that may be produced after the adsorbent reacts with the acids. By identifying the chemical processes that produce the

finished chloro- and fluoro- products, specifically by direct reactions of the solid adsorbent with HCl and HF. The adsorbent that is most suitable for the process in terms of cost and market for the final product may be determined. Most of the reactant and product prices indicated in this chapter are bulk shipping prices and are subject to change depending on the time of purchase and the quality of the chemicals needed.

## 3.1. FLUORINATED AND CHLORINATED COMPOUNDS

CFCs and HCFCs that are broken down generate a mixture of HCl and HF gases. An ideal solid adsorbent must therefore be capable of reacting with both gases under the same conditions at the same time. However, selective reactions between two different adsorbents and the gas mixture are also possible. The potential solid adsorbents discussed in this Section are the oxides, carbonates, sulfates or hydroxides of aluminum, calcium, sodium, magnesium, as well as iron and silicon. In addition, the properties of the products of their reaction with the acidic gases and the estimated adsorbent mass required to meet the target production capacity of the acidic gas are described.

### *3.1.1. Aluminum Fluoride ($AlF_3$)*

Aluminum fluoride is a stable compound suitable for this application if formed at the reactor temperatures. However, aluminum chlorides are highly reactive with water, and the corrosive properties of this material may result in accelerated wear of the reactor. Its major use is as a flux in the aluminum industry during electrolysis.[34–39]

$AlF_3$ is a non-toxic chemical unless heated to above 773 K (500°C) in the presence of moisture, at which time a pyrohydrolysis occurs with the evolution of hydrogen fluoride vapour, a respiratory irritant.[40] By using the HF-based chemical equation, 0.8494 g of adsorbent ($Al_2O_3$) is required per gram of HF adsorbed. The raw material is available in the USA, China, India, Taiwan and the UK.

Current industrial process

$$H_2SiF_6 + 2\ Al(OH)_3 + 2\ H_2O \rightarrow 2\ AlF_3 \cdot 3H_2O + SiO_2$$

HF-based process

$$Al_2O_3 + 6\ HF \rightarrow 2\ AlF_3 + 3\ H_2O$$

### *3.1.2. Aluminum Chloride ($AlCl_3$)*

Aluminum chloride reacts violently with water at room temperature to generate an acidic solution. It is used as a catalyst in chemical reactions and syntheses, the most important use being in Friedel–Crafts reactions in which the products are used in the manufacture of detergents and petrochemicals like alkyl and ethyl benzene. It reacts with water to form hydrogen chloride gas at ambient conditions.[41] Applying the HCl-based chemical equation, 0.4661 g of adsorbent per gram of HCl adsorbed is needed. The raw material is available in Canada, the USA and China.

Current industrial process

Chlorination of alumina at 800°C in the presence of a reducing agent carbon or carbon monoxide.

Alternatively, mix alumina with about 20 wt% of carbon and a small amount of sodium salt and chlorinate mixture at 600°C (the Bayer process).

HCl-based process

$$Al_2O_3 + 6\ HCl \rightarrow 2\ AlCl_3 + 3\ H_2O$$

*Market:*

Price of $Al_2O_3$ = US$ 0.31/kg [42]
Price of $AlF_3$ = US$ 0.270/kg [43]
Price of $AlCl_3$ = US$ 0.26/kg [44]

To neutralize a mixture of 7230 kg of HCl and 3970 kg of HF gas per month, about 6740 kg of aluminum oxide is required, resulting in a raw material cost of US$ 2,089.71 per month.

### *3.1.3. Fluorspar ($CaF_2$)*

Fluorspar is solid and stable at the reactor temperature. Calcium chloride which will be produced concurrently with calcium fluoride is also solid and stable around the reactor temperatures and can be separated from fluorspar based on their relative solubility in water or acetone. There are three principal types of industrial use for natural fluorite, corresponding to different grades of purity.[45–47] These are the metallurgical grade fluorite, the ceramic grade fluorite and the "acid grade fluorite". Fluorspar finds uses in metallurgy, the glass industry, dental applications, and the chemical industry, just to mention a few.[48] By applying the HF-based chemical equation, 2.5014 g of adsorbent is needed per gram of HF adsorbed. The raw material is available in Canada, the USA and China.

Current industrial process

Mined

HF-based process

$CaCO_3 + 2\ HF \rightarrow CaF_2 + H_2O + CO_2$

$CaCO_3 \rightarrow CaO + CO_2$ (at temperatures above 800°C)

### *3.1.4. Calcium chloride ($CaCl_2$)*

Calcium chloride is stable at high temperatures and more soluble in water than its fluoride equivalent. Thus, the two compounds can be easily separated if need be. It is used in dust laying, snow and ice control in highway maintenance; calcium salts production in the chemical industry and low alkali cement production in the cement

industry. It is also used in the food, construction, refrigeration, automotive and aluminum, mining, paper manufacturing, petroleum and agricultural industries. From the HCl–based equation, 1.3725 g of adsorbent/gram of HF adsorbed would be needed. The raw adsorbent is available in the USA and China.

Current industrial process

Solvay process: $2\ NaCl + CaCO_3 \rightarrow Na_2CO_3 + CaCl_2$

HCl-based process

$CaCO_3 + 2\ HCl \rightarrow CaCl_2 + H_2O + CO_2$

*Market:*

Price of $CaCO_3$ = US$ 0.06/kg [49,50]
Price of $CaF_2$ = US$ 0.27 to US$ 0.65/kg [51,52]
Price of $CaCl_2$ = US$ 0.1 to US$ 0.31/kg [49,53]

To neutralize a mixture of 7230 kg of HCl and 3970 kg of HF gas per month, about 19800 kg of calcium carbonate is required, resulting in a raw material cost between US$ 1,190.62 per month.

### *3.1.5. Sodium fluoride (NaF)*

Sodium fluoride, though stable at high temperatures, reacts with metals which causes corrosion. The bifluoride equivalent decomposes to yield NaF and hydrogen fluoride, which is also corrosive. Sodium fluoride is used in toothpastes and other dental hygiene products because fluoride effectively prevents dental decay. It is also one source of fluoride used in public water treatment systems.[54] It prevents the growth of bacteria, fungi and mold and for that reason, various types of adhesives and glues have sodium fluoride as a preservative to control decay.[55] Alternatively, sodium fluoride is used as a cleaning agent, e.g. as a "laundry sour".[35,56] By using the HF–based chemical equation, 1.9992 g of adsorbent is neutralized per gram of HF adsorbed for NaOH and 2.6489 g of

adsorbent per gram of HF adsorbed for $Na_2CO_3$. The raw materials are available in the USA, Canada and China.

Current industrial process

Same as direct fluorination

HF-based process

$$NaOH + HF \rightarrow NaF + H_2O$$

$$Na_2CO_3 + 2\ HF \rightarrow 2\ NaF + H_2O + CO_2$$

### *3.1.6. Sodium chloride (NaCl)*

Sodium chloride is readily prepared by the evaporation of brine and the mining of rock salt; it is not industrially produced through a chemical process. It is used in the chemical industry as a starting material for the synthesis of industrial chemicals. It is also used in the food, pottery and textile industries.[57]

Current industrial processes

Mined or produced by seawater evaporation.

HCl-based process that produces NaCl

$$NaOH + HCl \rightarrow NaCl + H_2O$$ (typically occurs in the liquid phase)

$$Na_2CO_3 + 2\ HCl \rightarrow 2\ NaCl + CO_2 + H_2O$$

*Market:*

Price of NaOH = US$ 0.10/kg [58]
Price of $Na_2CO_3$ = US$ 0.13/kg [49,59]
Price of NaF = US$ 0.50/kg [49,60]

To neutralize a mixture of 7230 kg of HCl and 3970 kg of HF gas per month, about 21000 kg of sodium carbonate is required, resulting in a raw material cost between US$ 2,732.97 per month.

### *3.1.7. Magnesium fluoride ($MgF_2$)*

Magnesium fluoride is a stable solid at the reactor temperatures. However, magnesium chloride is corrosive. It is used in windows, lenses, and prisms because it is transparent over a wide range of wavelengths.[61] It is tough, works and polishes well [35] and is a preferred material for UV laser use.[61] By applying the HF-based chemical equation, 3.0082 g of adsorbent is required per gram of HF adsorbed for $MgSO_4$ and 2.1072 g of adsorbent/gram of HF adsorbed for $MgCO_3$. The raw materials are available in China, India and Canada.

Current industrial process

$$CaF_2 + MgCl_2 \xrightarrow[(150-190°C)]{} MgF_2 + CaCl_2$$

HF-based process

$$MgSO_4 + 2\ HF \rightarrow MgF_2 + 2\ H^+ + SO_4^{2-}$$

$$MgCO_3 + 2\ HF \rightarrow MgF_2 + CO_2 + H_2O$$

### *3.1.8. Magnesium chloride ($MgCl_2$)*

Magnesium chloride is highly corrosive, despite its stability at the reactor temperatures. It is used in the production of magnesium metal, as a dust binder on roads, as a flocculating agent in water treatment, for dressing cotton and woolen fabrics, as a fire-extinguishing agent and fireproofing material, in sugar beet processing and as a catalyst.[57]

Current industrial processes

a) Treating seawater with lime or calcined dolomite.
b) $MgO + C + Cl_2 \rightarrow MgCl_2 + CO$

HCl-based process

$$MgCO_3 + 2\ HCl \rightarrow MgCl_2 + H_2O + CO_2$$

$$MgO + 2\ HCl \rightarrow MgCl_2 + H_2O$$

$$Mg(OH)_2 + 2\ HCl \rightarrow MgCl_2 + 2\ H_2O$$

*Market:*

Price of $MgSO_4$ = US$ 0.02/kg [49]
Price of $MgCO_3$ = US$ 0.075/kg [62]
Price of $MgF_2$ = US$ 0.65/kg [63]
An alternative raw material is $Mg(OH)_2$ which when heated generates MgO.

To neutralize a mixture of 7230 kg of HCl and 3970 kg of HF gas per month, about 16700 kg of magnesium carbonate is required, resulting in a raw material cost between US$ 1,254.59 per month.

### *3.1.9. Iron (II) fluoride ($FeF_2$)*

Iron (II) fluoride, when heated in the presence of oxygen, forms rust. It is used in the production of ceramics and as a catalyst.[57,64]

Current industrial processes

$$2\ FeF_3 + H_2 \rightarrow 2\ FeF_2 + 2\ HF$$

$$FeCl_2 + F_2 \rightarrow FeF_2 + Cl_2$$

HF-based process

$$Fe + 2\ HF \xrightarrow[\text{(high temperature)}]{} FeF_2 + H_2$$

### *3.1.10. Iron (II) chloride ($FeCl_2$)*

Iron (II) chloride occurs as the natural mineral lawrencite. The hydrated forms melt and vapourize at temperatures between 370 and 953 K. It is used as a mordant for dyeing and also in the pharmaceutical, sewage treatment and metallurgical industries.[57]

Current industrial processes

$$Fe + 2\ HCl \xrightarrow[(700°C)]{} FeCl_2 + H_2$$

$$Fe + Cl_2 \xrightarrow[(700°C)]{} FeCl_2$$

$$Fe + 2\ HCl + 4\ H_2O \xrightarrow[\text{(room temperature)}]{} FeCl_2 \bullet 4H_2O + H_2$$

HCl-based process

$$Fe + 2\ HCl \xrightarrow[(700°C)]{} FeCl_2 + H_2$$

Price of Fe = US$ 59/kg [65]
Price of $FeF_2$ = US$ 3.80/kg [66]
Price of $FeCl_2$ = US$ 0.25 /kg [67]

Considering the cost of iron metal and those of the products, it is not reasonable to use iron metal as a raw material. Iron (III) oxide may be a better replacement however it would result in the production of iron (III) salts.

### *3.1.11. Iron (III) fluoride ($FeF_3$)*

Iron (III) fluoride is a powerful dehydrating agent and its formation may be responsible for the explosion of a cylinder of fluorine gas. It is also not as useful as its chloride equivalent. It is used in the production of ceramics and as a catalyst.[68]

Current industrial processes

Treating any anhydrous iron compound with fluorine. (Usually the process is the same as HF–based process).

HF-based process

$$FeCl_3 + 3\ HF \rightarrow FeF_3 + 3\ HCl$$

### *3.1.12. Iron (III) chloride ($FeCl_3$)*

Iron (III) chloride occurs as the natural mineral molysite. The hydrated forms tend to melt and vapourize at much lower temperatures compared to the anhydrous forms. It is used in the preparation of iron (III) salts, in waste treatment processes, in dyes, pigments and inks manufacturing, as a chlorinating agent and as a catalyst.[57]

Current industrial processes

$$2\ Fe + 3\ Cl_2 \xrightarrow[(350°C)]{} 2\ FeCl_3$$

$$FeCl_3 \bullet 6H_2O + 6\ SOCl_2 \rightarrow FeCl_3 + 12\ HCl + SO_2$$

HCl-based process

$$Fe_2O_3 + 6\ HCl \xrightarrow[(elevated\ temperatures)]{} 2\ FeCl_3 + 3\ H_2O$$

Price of $Fe_2O_3$ = US$ 0.98/kg [49]
Price of $FeCl_3$ = US$ 1.00/kg [62]

## 3.2. PORTLAND CEMENT

A typical Portland cement composition is provided in Table 3.1., and will be used in the analysis of adsorption capacity and expected product composition.

**Table 3.1.** Typical Composition of Ordinary Portland Cement.[69,70]

| COMPOUND | % BY WEIGHT |
|---|---|
| $Ca_3SiO_5$ | 60 |
| $Ca_2SiO_4$ | 12 |
| $Ca_3Al_2O_4$ | 12 |
| $Fe_2O_3$ | 4 |
| MgO | 2 |
| $CaSO_4$ | 7 |
| $CaCO_3$ | 3 |

### *3.2.1. Fluoride content*

While the allowable fluoride content can range by application, typical values of 0.06, 0.2 and 0.4 wt% have been encountered for clinker obtained from cement production units.[71] Assuming 0.4% maximum Fluoride content in a Portland cement having the composition given above, fluoride ions would constitute 0.004 kg per kg of cement material following blending of highly fluorinated adsorbent with raw Portland cement.

### *3.2.2. Chloride content*

Calcium Chloride is typically added to cement kilns at a composition of approximately 1% by weight.[72,73] This corresponds to a 0.64% by mass chloride content in the final blended product. Chloride content would thus be 0.0064 kg per kg of cement material following the blending of a highly chlorinated adsorbent with raw Portland cement.

Portland cement may be considered the combined form of CaO, $SiO_2$, $Al_2O_3$, $Ca_2(Al_2O_3)Fe_2O_3$, some MgO and $CaSO_4$, and free lime in the form of carbonates, $CaCO_3$ ($CaO + CO_2$).[70] The extent to which these compounds can be fluorinated is not fully available in literature, and will likely be easier assessed during experiments. Nonetheless, for a preliminary assumption we may assume that the free lime and a CaO from $Ca_3SiO_5$ will react. Based on this assumption, 0.164 kg of CaO will be available to bond with fluorine or chlorine per kg of Portland cement. Upon complete reaction, this

would result in either 0.229 kg of $CaF_2$ or 0.325 kg of $CaCl_2$. The resulting material consumption would thus be:

17 g of Portland cement/ g of HF adsorbed, resulting in 18.1 g of fluorinated cement

9.4 g of Portland cement/ g of HCl adsorbed, resulting in 10.9 g of chlorinated cement

Based on the allowable fluoride and chloride contents, 1 kg of fluorinated cement would need to be blended with 250 kg of un-fluorinated Portland cement while 1 kg of chlorinated cement would need to be blended with 156 kg of Portland cement.

Furthermore, the direct fluorination of Portland cement may result in a wide variety of fluorides. In order to safely handle the off-gases from the reactor, it will likely be necessary to quench the solution in a caustic scrubber to remove fluorinated silicate gases.

There has been some interesting work done recently on the combination of fly ash, cement (white Portland, or Portland), and $CaF_2/CaCl_2$ to form stable building materials. $CaF_2$ may also be sold to cement kilns directly for addition to their cement mixtures at a rate of 3 to 5% by weight.

### 3.3. FLY ASH

Fly ash is produced when coal is combusted and, depending on the type of coal being burned, the percentage compositions of the constituent compounds will vary accordingly. Fly ash is typically made up of silica, aluminum oxides, iron (III) oxides and calcium oxides. Considering its use as a substitute for Portland cement and sand in concrete production, it is potentially a material worth mentioning for the intended purposes of acidic gas neutralization. It is anticipated that the various components will react with the acids to produce products that have been mentioned individually in previous Sections, i.e. silicon fluorides and chlorides, aluminum fluorides and chlorides,

iron fluorides and chlorides, and calcium chlorides and oxides. However, the resulting fluorinated and chlorinated compounds may not be easily separated for individual use.

The danger of fly ash is a result of its constituent compounds. Silica and lime are toxic chemicals and therefore their presence in fly ash renders it toxic to some extent. Also, their reaction with the acidic gases will produce toxic gaseous products mentioned in Section 2.3.1. and 2.3.2.

*Market:*

Price of fly ash: US$ 0.02.[74] There may be opportunities to work with the local power plants to obtain fly ash at a reduced rate.

### *3.3.1. Silicon tetrafluoride ($SiF_4$)*

Silicon tetrafluoride occurs as a gaseous substance which could be generated when hydrogen fluoride reacts with silicates. It is not the ideal product of choice after the adsorption process but is mentioned because silicates are present in both Portland cement and fly ash. It should also be noted that any quartz lining in the reactor may be subject to corrosion if $SiF_4$ is present. It is used in the electronics industry and in the production of other silicon compounds.[57]

Current industrial processes

$$2\ CaF_2 + 2\ H_2SO_4 + SiO_2 \rightarrow SiF_4 + 2\ CaSO_4 + 2\ H_2O$$

Heating of the hexafluorosilicate salts, preferably $Na_2SiF_6$.

HF-based process

$$SiO_2 + 4\ HF \rightarrow SiF_4 + 2\ H_2O$$

### *3.3.2. Silicon tetrachloride ($SiCl_4$)*

Silicon tetrachloride is produced as a gaseous substance. It is used in the preparation of pure silicon and organosilicon compounds and in smoke screen production.[57]

Current industrial processes

$$SiO_2 + C + 2\ Cl_2 \rightarrow SiCl_4 + CO_2$$

$$Si + 2\ Cl_2 \rightarrow SiCl_4$$

HCl-based process

$$Si + 4\ HCl \rightarrow SiCl_4 + 2\ H_2$$

## 3.4. SUMMARY OF ESTIMATED ADSORBENT USE FOR THE AMOUNT OF HF AND HCl PRODUCED

The values provided in Table 3.2. are approximate, and are only meant to provide an order of magnitude example of the expected quantity of solids needed. The high values observed for cement are likely an overestimate for the actual solids handling within the facility as the silicates and alumina fractions are likely to react and increase the adsorption capacity. Prices should be taken as approximate, as some were obtained from dated sources and others have purity constraints.

**Table 3.2.** Select Adsorbent Usage Based on 7230 kg HCl and 3970 kg HF Produced Each Month.

| RAW MATERIAL | PRODUCT | MONTHLY CONSUMPTION kg raw material | COST OF RAW MATERIAL * US $ | PRODUCT PRODUCTION kg of product | PRODUCT REVENUE * US $ |
|---|---|---|---|---|---|
| **$Al_2O_3$** | $AlF_3$<br>$AlCl_3$ | 3,373 | 2,092 | 5,556<br>8,822 | 1,500<br>2,294 |
| **$CaCO_3$ (Limestone)** | $CaF_2$<br>$CaCl_2$ | 9,933 | 1,192 | 7,748<br>11,014 | 2,092<br>1,102 |
| **$MgSO_4$** | $MgF_2$ | 11,945 | 239 | 6,183 | 4,019 |
| **$MgCO_3$** | $MgF_2$<br>$MgCl_2$ | 8,367 | 1,255 | 6,183<br>9,449 | 4,019<br>473 |
| **$Fe_2O_3$** | $FeF_3$<br>$FeCl_3$ | 5,282 | 5,177 | 7,465<br>10,731 | -<br>10,732 |
| **Portland Cement** | 0.4% F content<br>0.6% Cl content | 67,490<br>67,962 | 8,127 | 71,857<br>78,807 | ** |
| **Fly Ash** | $SiF_4$<br>$SiCl_4$<br>$AlF_3$<br>$AlCl_3$<br>$FeF_3$<br>$FeCl_3$<br>$CaF_2$<br>$CaCl_2$ | Variable, likely on the range of 10,000 | - | - | - |

*The prices in these columns are based on the prices mentioned in Sections 2.1 to 2.3 of the raw materials and products; and the monthly mass consumption of the raw material and product generated.

**This material would need to be blended with approximately 18,000 metric tonnes of raw Portland cement per month to meet the maximum fluorine and chlorine content.

## 3.5. RECOMMENDATIONS

The utility to use locally available media in the neutralization of the acidic gases, e.g. Portland cement, fly ash and limestone should be investigated further.

Portland cement was identified in the project scope as a material of specific interest, but a useable product would require subsequent blending with a fairly large

quantity of non-fluorinated cement to meet maximum fluoride and chloride content specifications. The prospects of re-selling a finished product back to the cement industry vs. selling a fluorinated raw material are also lower. While potentially feasible, it would make more sense to produce either a $CaF_2/CaCl_2$ mix for sale to the concrete industry, or a fluorinated fly-ash mixture.

There are a number of advantages to producing $CaF_2$ and $CaCl_2$ relative to the other options currently considered: common raw material (limestone, powdered or granular), very low fluorinated product solubility in water (good for long term storage and handling), ease of separation (precipitating $CaF_2$ product with $CaCl_2$ in solution if using wet quench, or an electrostatic precipitator for a dry system), and multiple end-point potentials (concrete industry, solid sequestration with concrete and fly ash, other areas depending on purity produced). Powdered limestone can also be purchased fairly cheaply ($40 to $100/tonne), corresponding to a raw material cost of ~$0.16 per kg of refrigerant decomposed if the theoretical adsorption capacity is attained.

If the desire is to produce something with a greater market in the cement industry, fluorination of fly ash may be another good alternative. Potentially available from the local power plant, fly ash is currently used as a filler in many cement mixtures. There are, however, technical considerations that may limit this approach for this application (similar to those that would be encountered with Portland cement). Due to the high silicate content, it is likely that appreciable quantities of $SiF_4$ will be generated, requiring the use of a caustic scrubber downstream of the reactor. While this may be necessary even with the limestone system, the load on the limestone system would be minimal relative to that expected if $SiF_4$ were generated in appreciable quantities.

In this project, limestone was studied as a suitable adsorbent, followed by a mixture of finished cement product (i.e. Portland cement) and limestone.

# 4. EXPERIMENTAL SETUP & SYSTEM OPERATION

The experimental setup for the neutralization of hydrochloric and hydrofluoric acids at 408 K (135°C) with limestone was used to study the reaction process, by exposing the limestone particles to the acidic gases in a packed bed reactor. The data gathered from the experimental runs were analyzed using the shrinking core model which provided information on the efficiency of the neutralization process, as well as the estimated time for complete particle consumption.

The schematic diagram of the experimental setup is shown in Fig 4.1.

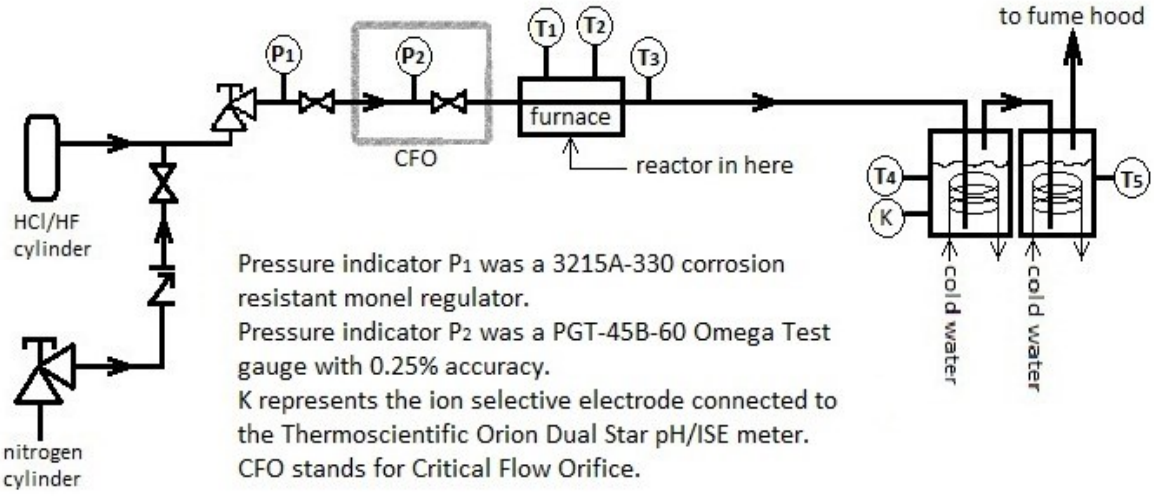


**Figure 4.1.** Schematic diagram of the acidic gas neutralization system using solid adsorbents.

## 4.1. MAIN COMPONENTS OF THE EXPERIMENTAL SETUP

This Section describes the experimental system, detailing its main components as shown in Fig 4.1. The nitrogen cylinder was used to calibrate the critical flow orifice (CFO) and also to purge the entire system before and after acidic gas runs. The HCl/HF cylinder provided 5% HCl/HF acids for the required runs, pressure indicators $P_1$ and $P_2$ were used to measure and monitor pressure changes during the experimental runs and thermocouples $T_1$, $T_2$ were used to measure and monitor the temperature of the furnace and $T_3$, $T_4$, $T_5$ that of the effluent gases. All pipes, valves and fittings connected to the

first neutralization bath were made of Inconel, except the flexible PFA tubing connecting the nitrogen cylinder to the check valve. All pipes and fittings after the first bath were made of stainless steel and Tygon tubing connected cold water from the tap to cooling coils and also carried off-gases to the fume hood. The ion selective electrode was inserted into the first neutralization reservoir to measure changes in chloride or fluoride ion concentration for the HCl and HF gas runs respectively. Cooling water was fed to the system via the cooling coils within the neutralization.

When the gas cylinder and valves were opened, the gas flowed through the critical flow orifice (CFO). The CFO was used to estimate the incoming gas flow rate. it consists of a Monel104 miniature needle valve which was set up as a CFO and calibrated using nitrogen gas. The coefficient of flow ($C_v$) for the CFO was calculated using eqn. 4.1.[75]

$$C_v = Q_G \frac{\sqrt{(S.G \times T)}}{816 \times P_1} \tag{4.1}$$

Where $Q_G$ is the Gas Flow rate in Standard Cubic Feet per Hour = $7.1\times10^{-6}$ $m^3/s$ = 0.9026 scf/hr at standard temperature and pressure (STP), *S.G* (Specific Gravity) of HCl at STP = 1.268 (where air at STP = 1.0), *T* (Absolute temperature) in ºR = 293.15K = 527.67°R and $P_1$ (inlet gas pressure for critical flow) = 241.32 kPa = 49.7 psia. The coefficient of flow $C_v$, therefore becomes:

$$C_v = 0.9026 \times \frac{\sqrt{(1.268 \times 527.67)}}{816 \times 49.7} = 0.00058 \tag{4.2}$$

For critical flow, the pressure before the CFO ($P_1$) must be at least two times greater than the pressure after the CFO ($P_2$); i.e. $P_1 > 2P_2$.[75] When $P_1$ is greater than the critical flow pressure, the flow rate is independent of $P_2$.[76]

The needle valve was set to operate as a CFO for a flow rate of $7.1\times10^{-6}$ $m^3/s$, using the calibration determined from an Omega rotameter with model number FL-3802ST. The pressure reading corresponding to the flow rate was obtained via a calibration chart (Fig 4.2.) which was plotted by relating the scale reading and flow rate

from the manufacturer's calibration data (Appendix A2.) to the scale reading and corresponding pressure measured on $P_1$.

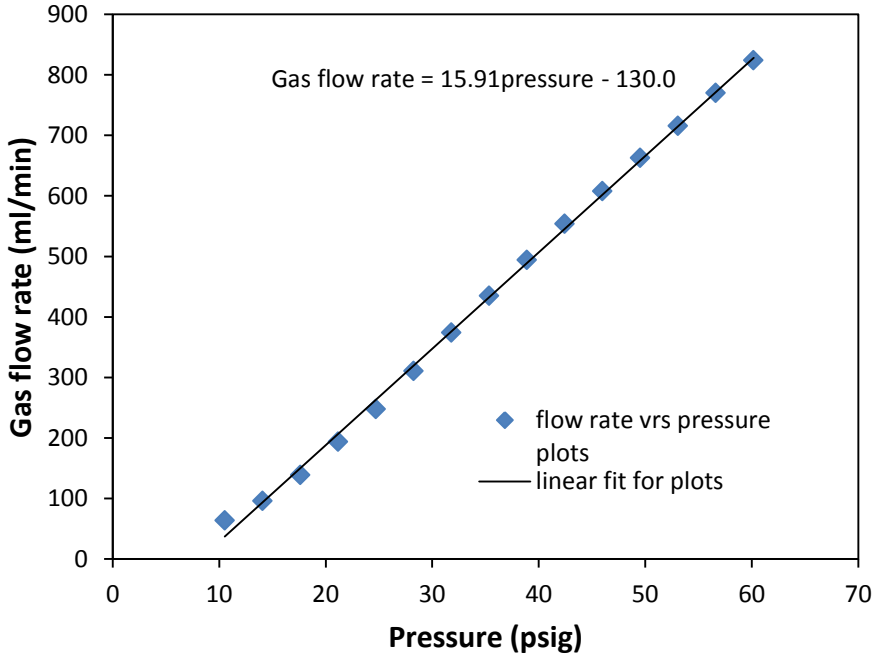


**Figure 4.2.** Calibration chart for the CFO obtained using nitrogen gas.

As the gas flowed through the packed bed, a change in its flow properties was expected. The Ergun equation (eqn. 4.3) provides information on the changes in the acidic gas properties as it flows through the packed bed. It was used to calculate the pressure drop across the bed.

$$\frac{\Delta P}{L} = \frac{150\mu(1-\varepsilon)^2 u_0}{\varepsilon^3 d_p^2} + \frac{1.75(1-\varepsilon)\rho u_0^2}{\varepsilon^3 d_p} \tag{4.3}$$

Where $\Delta P$ = pressure drop in Pa, $\varepsilon$ = bed void space, $L$ = height of bed in meters, $\mu$ = fluid viscosity in Pa·s, $u_0$ = fluid superficial velocity in m/s, $d_p$= particle diameter in m and $\rho$ = fluid density in kg/m$^3$. For a bed of length 0.0254 m, filled with 0.001 m diameter particles in a 0.4 bed void space, having a fluid with viscosity $2.286\times10^{-5}$ Pa·s, a fluid density of 2.114 kg/m$^3$ and a superficial fluid velocity of 0.0561 m/s (based on 0.00635 m internal reactor radius), the change in pressure $\Delta P$ becomes:

$$\frac{\Delta P}{0.0254} = \frac{150(2.286\times10^{-5})(1-0.4)^2(0.056)}{(0.4)^3(0.001)^2} + \frac{1.75(1-0.4)(2.114)(0.056)^2}{(0.4)^3(0.001)}$$

$\Delta P = 21.1$ Pa

The change in pressure was calculated to be approximately 21 Pa, and since this value was very small, it was safely assumed that the pressure drop across the bed was negligible. Thus the upstream pressure (pressure of the gas as it flows to the packed bed) was approximately the same as the downstream pressure (pressure of the gas as it flows out of the packed bed).

The reactor was filled with 7.3209 ± 0.0070 g of limestone particles. The mass of the adsorbent was measured by filling the reactor with the adsorbent such that the reactor could be safely closed without any further crushing of the particles. After this, the particles were poured out into a weighing bowl and weighed using a Sartorius CP 124S mass balance with ±0.0001 g accuracy. A Deacon 8875-Thin high temperature sealant was applied to the reactor threads to ensure a leak-proof seal, and the reactor pieces were screwed together to form a single unit. The unit was then placed in the ceramic piece and placed in the electric furnace to cure.

A John Deere electric furnace (model number 2238-24-3ZH) with a maximum operating temperature of 1477.15 K (2200°F, 1204°C) was used in this study. In this investigation, it was operated at 523.15 K (250°C) above which the Deacon 8875-Thin high temperature thread sealant oxidized. At this operating temperature, the temperature of the gas exiting the reactor was measured by the automatic temperature scanner (Omega, DP1001AM) to be between 403.15 and 413.15 K (130 and 140°C). Details on the operation of this furnace are found in Appendix A3.

As the gas flowed through the cylindrical tube of the reactor, it was heated and reacted with the adsorbent. Any unreacted gas exited the reactor and entered the neutralization reservoirs where they were neutralized by the neutralization solution.

The neutralization reservoirs neutralized any unreacted incoming acidic gases exiting the reactor, with a 2.5 L solution of 0.0374 M sodium bicarbonate (Arm and

Hammer baking soda) for the HCl runs and a 2.5 L solution of a mixture of 0.0374 M sodium bicarbonate and 0.0374 M limestone each for the HF runs (see Appendix A4. for how this was calculated).

The first reservoir was equipped with either a Cole Parmer Instruments' chloride or fluoride ion selective probe (with model numbers K-27502-07 and K-27502-19 respectively) to detect and measure the chloride or fluoride ion concentration depending on which acidic gas was being employed. The probes were connected to a Thermo Scientific Orion Dual Star $^{TM}$ pH/ISE meter with model number E05289 which was used to record the measurements. The probes were calibrated only once at the beginning of the runs. Calibration details of these probes are found in Appendix A5.

Both reservoirs were also equipped with Teflon coated magnetic bars rotated by a Thermoscientific Variomag mono direct stirrer to ensure active mixing of the incoming gas. The increased agitation provided by the presence of the stir bars enhanced mass transfer between the sparging gases and the neutralization solution. This proved to be efficient because the effluent gases exiting the neutralization reservoirs were not found to contain HCl or HF by the Honeywell MDA Scientific Midas gas detector. Each neutralization reservoir was equipped with a cooling water loop which kept the temperature of the neutralization solutions cool and the temperatures were monitored using thermocouples.

## 4.2. TYPICAL RUN PROCEDURE

For a single run, taking into consideration the preparation and cleaning after the experiment, a total of two days was required. The time for the actual runs of the acidic gases varied among an hour, an hour and a half, and a maximum of three hours. Adding time for nitrogen purges, this lasted about an hour before the acidic gas runs and up to three hours after the acidic gas runs, brought the range of total time required between three hours and seven hours. The process for running the entire system is described in a systematic order in the Fig 4.3.

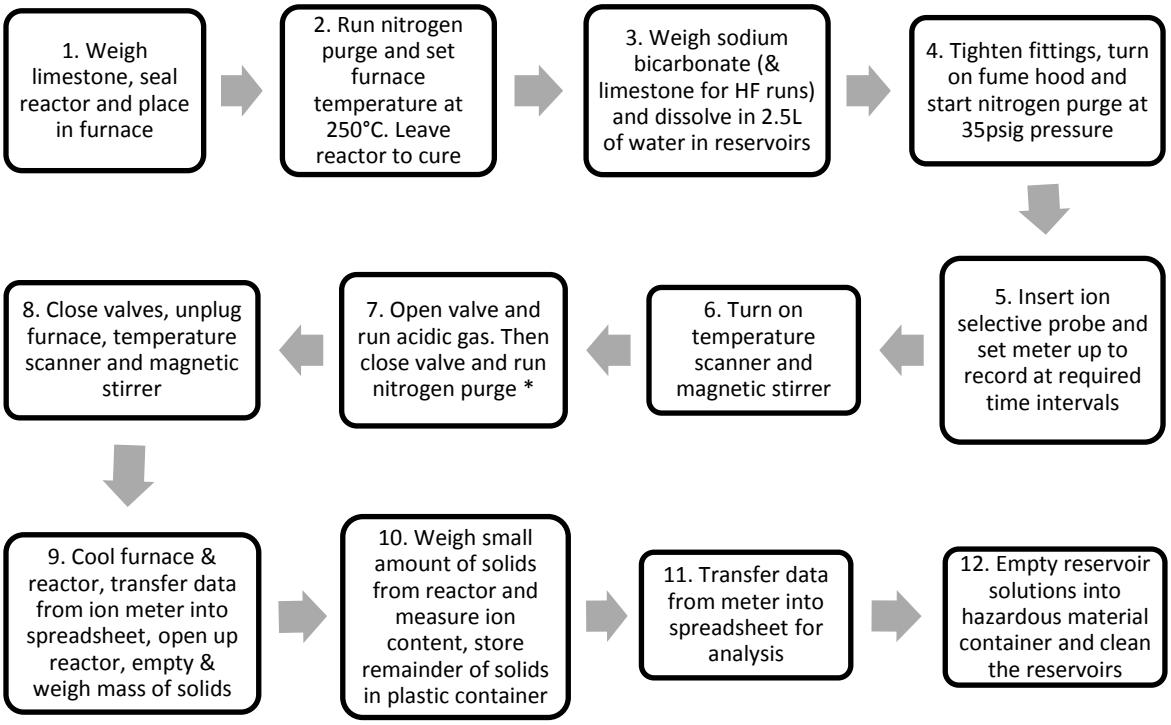


*For the pulsed injection, this was conducted within two minutes; however, for the continuous runs, the time between running the acidic gas and running the nitrogen purge ranged from 1 hour to 2.5 hours.

**Figure 4.3.** Step-by-step description of a typical experimental run.

A day before an actual run, steps 1 and 2 were performed using approximately 7.3209 ± 0.0070 g of limestone and connecting the top and bottom fittings to the reactor. Step 3 was conducted by taking the neutralization reservoirs lids off and putting them back on after the experiment was completed.

On the day of the run, after all safety apparel, which included a lab coat, safety glasses, gas respirator and hand gloves, was put on, the fittings connecting the piping to the first neutralization reservoir were fixed and tightened. Steps 4, 5 and 6 were carried out and at 5 to 10 minute intervals the pressure was recorded to provide information on the pressure drop as the flow continued. The ion selective probe was set up to record at 15 second intervals (refer to Appendix A6.) for all the runs except the three hour HF run for which recordings were at 30 second intervals. This was because the meter has the capacity to store up to 1000 recordings after which it overrides the previous

measurements or ceases to record further. A five hour total run with measurements at 15 second intervals would exceed the 1000 points available, resulting in data loss.

Step 7 was performed. The time, starting pressure and changes in pressure at varying time intervals were noted until the end of the run. It must be noted that the respirator was kept on throughout the duration of the entire run.

At varying time intervals for the pulse and continuous runs, the meter readings from the probe were observed and if they exceeded the 100 ppm point, the acidic gas cylinder was shut off and the nitrogen purge started again until the meter readings stabilized, i.e. no further changes in the concentration values occurred. The purge was run between an hour and three hours depending on the rate at which the meter readings stabilized.

Steps 8 and 9 were then carried out. The furnace door was opened to aid with the cooling process. In some cases, the furnace was left overnight to cool. After the reactor was cooled, the fittings were loosened and taken off, the reactor sent to the workshop to be opened up using a wrench and bench vice. The solids inside were carefully poured out into a weighing bowl, weighed and the mass noted.

Step 10 was performed by weighing 1.0031 ± 0.0091 g of the reactor solids from the HCl run, crushing them in a crucible and dissolving them in 75ml of deionized water. The ISE probe was placed in the resulting solution and the chloride ion concentration measured at one minute intervals. This process was repeated two more times and the results noted in each case. Using simple ratio and proportion, the amount of chloride ion in 7.3208 ± 0.0070 g of limestone was then estimated. For the HF run reactor solids, 0.0066 ± 0.0012 g of the crushed solids was dissolved in 500 ml deionized water. Just as in the case of the chloride ion determinations, the probe was inserted and measurements noted at one minute time intervals. The process was repeated twice more, the results recorded, and the fluoride content for 7.3208 ± 0.0070 g of solid estimated. The mass of reactor solids used to estimate the ion content was much lower in the case of the HF runs because of the relatively lower solubility of calcium fluoride in water compared to that of calcium chloride. To ensure that all the calcium fluoride present in the reactor solids

completely dissolved in a larger volume of water (500 ml), a smaller mass of the solids needed to be added.

Step 11 was conducted via a computer connection and the transferred results were then used to approximate the amount and fraction of the solid particles that had reacted. This data was used to estimate the effective diffusivity of the gases into the solid and consequently the length of time required for the solids to efficiently neutralize the gases under the experimental conditions.

Step 12 was carried out to safely dispose of the chlorinated/fluorinated neutralization solution. The emptied reservoirs were then rinsed clean and placed in the fume hood.

## 4.3. SYSTEM COMMISSIONING AND OPERATION

To ensure that the system was leak–proof, a nitrogen purge was run through it and the neutralization reservoirs were observed for bubbles. Subsequently, before the acidic gases were run, the system was checked for leaks by watching out for foaming after applying soapy solution to the connections and flowing nitrogen gas through the system.The connections that were observed to be leaking were taken apart and reconnected. The leak testing was repeated again to ensure that there were no more leaks. The leak testing procedure was necessary because any leak of the hazardous acidic gases as they were being run was dangerous. The reactor unit however could not be leak tested using the aforementioned method because after cooling the unit from 523 K (250°C), the sealant had expanded and contracted, making it predisposed to leaks.

A Honeywell MDA Scientific Midas gaseous HCl detector (model number MIDAS-E-HCl) was used to detect any leaks of the acidicgases along the entire system during the actual gas runs. A connecting tube that was moved along the system when the acidic gases were run, sucked air into the unit, which displayed a measurement in parts per million (ppm). The detector had a detection range between 0–8 ppm and upon detection of gas concentrations above 8 ppm an alarm went off, drawing attention to the

leaking hazard. The cylinders were then shut off immediately. This detector was also used to detect HF gas during the HF runs, though it was overly sensitive to the HF gas as mentioned by the manufacturer. To mitigate the risk of operator exposure, the neutralization reservoirs were placed in a fume hood. A gas respirator was worn during the entire duration of all the experimental runs and there was restricted access to the lab during the operation.

## 4.4. SAFETY CONSIDERATIONS

The gas detector was on during the entire time the experiments were conducted. During the initial commissioning of the system using HCl gas, a small leak between the cylinder and regulator connection was detected by the gas detector. As this was a CG-580 fitting with a compressed Teflon washer, the leak was attributed to insufficient compression of the washer. Following a minor adjustment of the coupling nut, no leaks were detected in any subsequent experiments.

A ceramic tube housing was placed inside the furnace to prevent contact between the metal reactor and the electric heating elements. The ceramic tube does not prevent the reactor from heating up; since there is heat convection, the reactor heated up and so did the gas as it flowed through the reactor.

Furthermore, holes were punched into the lids of the reservoirs to connect the two reservoirs, to transport cooling water in and out of the system and to carry gases out of the reservoirs to the fume hood. Teflon washers were placed both above and below the holes made in the lids before Swagelok fittings were put in place, to ensure that the seals were leak–proof for the HCl runs. For the HF runs, the Teflon washers were taken off and an epoxy adhesive was applied in its place to leak–proof the connections. Incoming connections from the reactor transported the gases into the first reservoir. Also, the second reservoir was a last resort to neutralize any incoming acids before the gases exited to the fume hood. In the worst case scenario, where the first reservoir got saturated and exceeded its capacity to neutralize any incoming gases, the second reservoir functions just like the first and reacts with the acids to neutralize them.

In order to always have an excess of sodium bicarbonate solution in the reservoirs during the runs, the required concentration was pre-calculated as described in Appendix A4. In addition, at no point during the entire experiment were both nitrogen and HF cylinders open at the same time. This prevented flooding of the HF cylinder, which was initially shipped with a maximum pressure of 150 psig, by the purging nitrogen cylinder, whose regulator was set to 200 psig. A flood of the cylinder would have altered the 5% composition of the HF gas and resulted in significant difficulty in determining HF adsorption fractions and parameters within the shrinking core model.

## 4.5. EXPERIMENTAL PLAN

Mosher limestone was obtained from a local store and the solid structure was characterized first by using simple wire meshes to obtain solid particles with approximate radius sizes between $0.298 < R < 0.584$ mm, $0.584 < R < 0.625$ mm and $0.625 < R < 1.18$ mm. The solids were well dispersed and not clumped together, which showed that the sieving technique employed for the particle size measurement was suitable.[77]

The HCl runs were conducted before the HF runs. The HCl cylinder had a pressure of 2000 psig. Three particle size ranges were studied for the HCl runs and the gas was fed initially as individual pulses and subsequently as a three-pulse run. The pulse runs were conducted by opening and closing the HCl cylinder within less than a minute, opening the valves for the gas to flow into the reactor and opening the nitrogen valve to purge the system after the pressure indicator began to drop. The nitrogen purge was run until the readings on the meter stabilized. The process was repeated twice more to obtain a three–pulse run. Though the actual gas pulse lasted less than a minute, it took approximately four minutes for all the gas to flow into the reservoir before the nitrogen purge was run. This delay was due to time it took for the gas to flow through the pipes, into the reactor, through the packed bed, through the pipes and into the neutralization reservoir where it was detected by the probe meter. For the initial test runs, the limestone in the $0.584 < R < 0.625$ mm particle size range was used. To also ensure that the system was safe, the gas detector was used to detect any leaks along the experimental setup

during the gas pulse. After the initial pulse runs, a three-pulse run was carried out using the narrower $0.584 < R < 0.625$ mm particle size range, followed by the $0.298 < R < 0.584$ mm and the $0.625 < R < 1.18$ mm ranges.

For the HF runs, only the narrower $0.584 < R < 0.625$ mm limestone particle size range was used. Additionally, continuous runs were conducted and the length of time of gas exposure to the particles in the reactor was varied between an hour and an hour and a half. In addition to the narrow limestone particles, a single run using a 50:50 mixture of limestone and cement powder was conducted to compare the capacity and efficiency of the two adsorbents. Similarly for safety, the gas detector was used to detect any leaks along the experimental setup. The results from all the runs were analyzed using shrinking core model kinetics which is discussed in Section 2.2. of Chapter 2.

# 5. RESULTS AND DISCUSSION

The results obtained from the HCl and HF runs indicate that approximately 49% of the fed HCl and between 7.8 – 16.2% of the fed HF gases reacted with the limestone particles in the reactor. The effective diffusivities of the HCl and HF gases into the limestone particles were estimated to be $1.5 \times 10^{-9}$ $m^2/s$ and $2.2 \times 10^{-9}$ $m^2/s$ respectively at 408 K (135°C), and $5.61 \times 10^{-9}$ $m^2/s$ and $8.24 \times 10^{-9}$ $m^2/s$ respectively at microwave plasma temperatures of 873 K (600°C). These effective diffusivity values result in complete particle consumption times of 227 hours and 154 hours for HCl and HF respectively at the experimental conditions, and 61 hours and 41 hours respectively under the microwave plasma conditions. Cement powder was found to adsorb only 0.65% of the fed HF gas when compared to the 1.16% adsorbed by limestone under the same experimental conditions.

## 5.1. PARTICLE CHARACTERIZATION

To facilitate the use of the shrinking core model for the effective diffusivity estimations (see eqn. 2.9), the required parameters were assumed as follows. The molar density of $CaCO_3$, $\rho_B$ in $mol/m^3$ particle had a value of 14992 $mol/m^3$ $CaCO_3$. This was based on a limestone density of 1501 $kg/m^3$, which was estimated by adding a known mass of limestone to a known volume of water and noting the change in volume; and a molar mass of $CaCO_3$ of 0.100 kg/mol. Since the measured density represented the particle density, $\phi_C$ was set equal to 1. Since two moles of acidic gas react with one mole of solid, the stoichiometric coefficient $b$ of the solid in the chemical reaction had a value of 0.5. The bulk phase concentration of HCl or HF, $C_{As}$, (assumed to be constant at 5% by volume at a pressure of 101325 Pa and a temperature equivalent to that of the effluent gas) had a value of 1.5 $mol/m^3$, and $r_c$ and $R$, the unreacted front position and outer radius of the particle, respectively were estimated from the volume of particle reacted via the measured chloride/fluoride ion content of the solids.

## 5.2. ANALYSIS METHODOLOGY

The breakthrough curves ranged from the period of time when the acidic cylinder was opened and closed, the nitrogen purge run, up until all the acidic gas had flown out of the system and the curve leveled off (see Fig 5.1.). From the typical breakthrough curves obtained from the runs, the maximum amount of fed gas that entered the neutralization reservoir was estimated by averaging the last 10 points at which the breakthrough curve leveled off. Fig 5.1. shows an example of this process from the HCl runs.

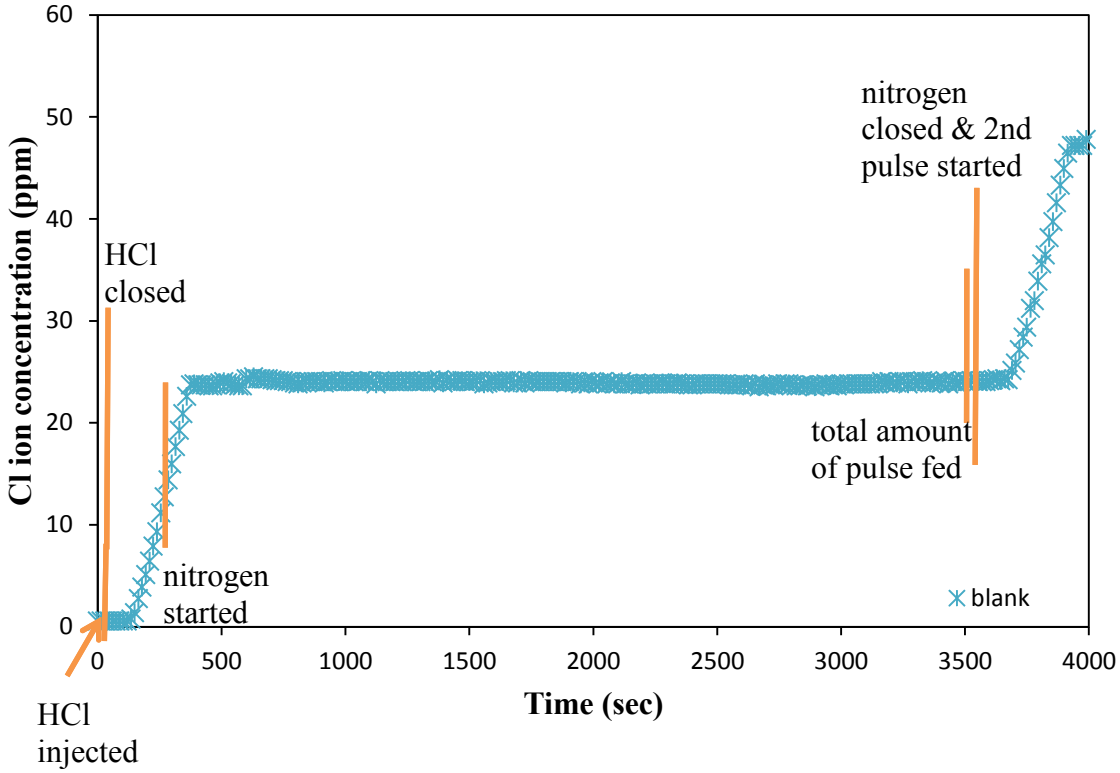


**Figure 5.1.** First pulse of the breakthrough curve for a blank run showing important points along the runs.

In the case of the HCl pulse runs, for the maximum amount that entered the reservoir at the end of each pulse was also estimated. The chloride and fluoride ion content of the limestone from the reactor was also estimated as described in Section 4.2. and this value in the case of the HCl runs was the total amount of fed acidic gas that

reacted after three pulses. Over the three pulses, the total amount of gas exiting the reactor was measured; this value when added to the total amount of reacted ions in the solids resulted in a value representing the total amount of HCl fed into the system. To estimate the amount of gas that reacted for each pulse, the ratios obtained from the blank runs were applied to the total amount of fed HCl. Knowing the amount fed for each pulse and the total amount exiting the reactor for each pulse, the amount of gas that reacted with the solids for each pulse was estimated.

## 5.3. RESULTS FROM EXPERIMENTAL RUNS AND ANALYSIS

### *5.3.1. Limestone and Cement Adsorbent Mixture Run*

To evaluate the feasibility of an alternative adsorption medium, one experiment was performed using a 50 wt% limestone, 50 wt% Portland cement mixture within the reactor, with a total solid mass comparable to previous experiments (~7 grams). The mixture was employed since the cement itself was a very fine powder that could not be supported on its own within the reactor (a fully packed reactor would become plugged).

During a 99 minute continuous HF flow test, the total amount of HF adsorbed by the solids in the reactor was approximately 1.81% of the HF fed (compared to between 15% and 18% for equivalent runs using limestone only). Of the 1.81% adsorbed by the solids, 1.16% was adsorbed by the limestone and only 0.65% was adsorbed by the cement powder. Despite the fact that the reduced cement particle size (on the order of microns) should have resulted in a significant fraction of the HF being adsorbed into the cement matrix, the actual amount adsorbed was significantly lower than the amount adsorbed by the comparatively larger limestone particles. This is likely due to the limited capacity of the cement, a value that is difficult to model considering that cement is made up of various metals and salts in differing compositions which will react with acidic gas to some extent. Furthermore, without a detailed compositional analysis of the cement's chemical makeup, it becomes difficult to estimate which components are reacting with the gas and what products they form. In addition, it seemed the presence of the cement powder together with the limestone decreased the ability of the limestone to react with

the gas. Perhaps, the powdery nature of the cement powder coated the limestone particles, reducing the amount of surface available for contact with the gas, resulting in the observed drastic reduction in HF neutralized (see Fig 5.2.).

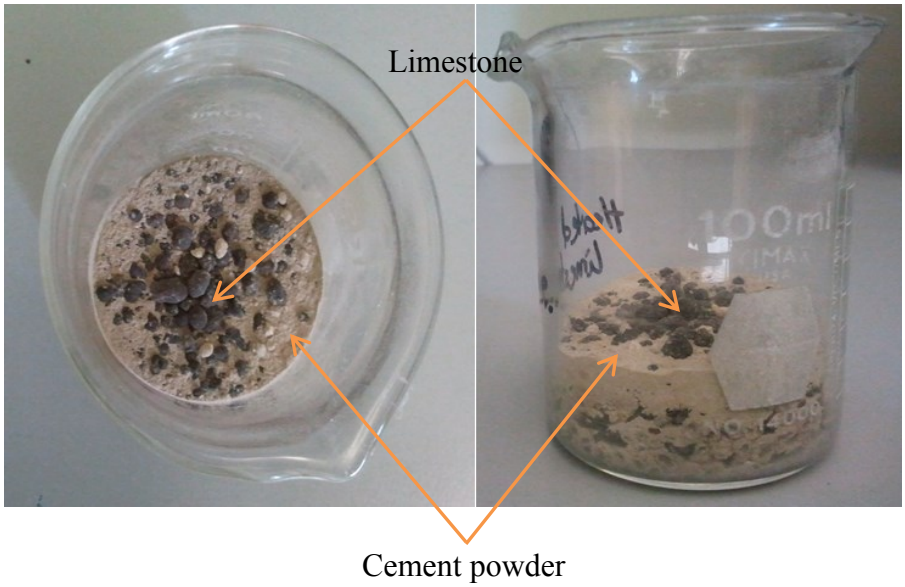


**Figure 5.2.** Images of the mixture of limestone and cement after the experimental run showing the variation in particle size between the cement and limestone particles.

Given the difficulty associated with handling solid media within a process environment, the increased volume of cement that would be required relative to that of limestone (and potential issues with exceeding permissible fluoride levels) may make this material unattractive as an adsorbent media. Subsequent runs therefore focused solely on using limestone particles as the preferred adsorbent.

### *5.3.2. Limestone as a Solid Adsorbent*

#### *5.3.2.1. HCl Gas as Adsorbate*

The HCl gas was fed to the limestone bed in pulses as described in Section 4.2. of Chapter 4. A blank run where the reactor was not filled with any limestone particles was conducted and the amount of acidic gas flowing through the system per pulse was estimated to be a 33%, 34% and 33% for the first, second and third pulses respectively

for a total HCl amount of 0.0052 moles. Four runs were then conducted after filling the reactor with about seven grams of limestone particles with particle radii in the ranges $0.298 < R < 0.584$ mm, $0.584 < R < 0.625$, $0.625 < R < 1.18$ mm and a blank run. Typical results from these runs are shown in Fig 5.3.

From the breakthrough curves, the amount of HCl gas that did not react with the limestone was obtained. This amount, together with the amount of chloride ions within the limestone particles gave the estimated amount of HCl gas that flowed through the system to be ~0.0101 ± 0.0010 moles during the entire 13 minutes that the gas was flowing (summing up the flow times for all three pulses).

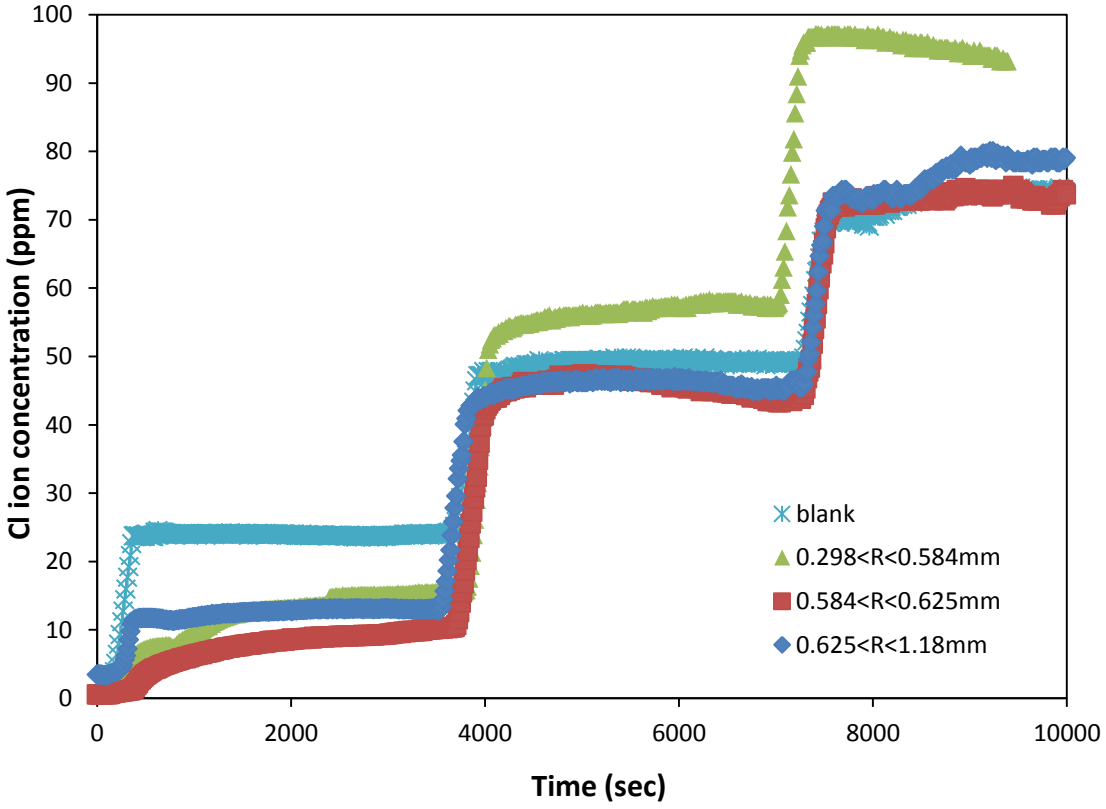


**Figure 5.3.** Typical breakthrough curves for HCl runs using the particle size ranges $0.298 < R < 0.584$ mm, $0.584 < R < 0.625$ mm and $0.625 < R < 1.18$ mm and a blank run.

Using the pulse ratios obtained from the blank runs, the estimated amount of HCl gas that flowed for each pulse was found and the amount of limestone that reacted per pulse was estimated to be 0.0026 moles for the first pulse, and 0.001 moles for each of the second and third pulses, resulting in a total limestone chloride ion content of ~0.005

moles. The amount of HCl gas that reacted out of the total amount fed for each pulse was also found to be ~73%, 29% and 29% respectively for the three pulses. This amount was estimated using an average of 10 final stabilized data points up to the total amount of pulse fed and back-calculated (see Fig 5.1, the 10 points were between the total amount of pulse fed and the point where the nitrogen was closed). It was observed that the first pulse consistently had the highest amount of gas reacting, mainly because there was no solid product layer on the outside of the solid and therefore there were no diffusivity limitations to slow down the reaction rate. For the second and third pulses however, the gas had to diffuse through the outer product layer into the unreacted core and therefore the reaction process was slowed down considerably.

The total amount of limestone consumed by the acidic gas was estimated using the measured chloride ion concentration (see Chapter 4, Section 4.2.) of the dissolved solids, and the balanced chemical reaction between calcium carbonate and HCl; this was found to be ~6.4%. This was based on the assumption that 20% of the solid limestone was present as elemental calcium (as indicated by the manufacturer of the limestone) and that the chloride ions that reacted would be present as calcium chloride.

Assuming that the particles were spherical, the Shrinking Core Model (SCM) described earlier was used to estimate the effective diffusivity values of the HCl-nitrogen mixture into the limestone particles and the results are shown in Table 5.1. The time values represent the time it takes for the pulsed HCl gas to completely flow through the system. These were estimated from the breakthrough curves obtained.

**Table 5.1.** Effective Diffusivity ($D_e$) Estimation from Experimental Data Using the SCM

| **Particle size radius (mm)** | **Time (sec)** | $D_{e\ \text{avg}}$ **($m^2/s$)** | $D_{e,\ \text{lower end radius}}$ **($m^2/s$)** | $D_{e,\ \text{higher end radius}}$ **($m^2/s$)** |
|---|---|---|---|---|
| **$0.298 < R < 0.584$** | 300 | $7.89\times10^{-10}$ | $3.59\times10^{-10}$ | $1.39\times10^{-9}$ |
| **(Smaller particles)** | 600 | $8.87\times10^{-10}$ | $4.04\times10^{-10}$ | $1.56\times10^{-9}$ |
| **$0.584 < R < 0.625$** | 400 | $1.42\times10^{-9}$ | $1.33\times10^{-9}$ | $1.52\times10^{-9}$ |
| **(Medium particles)** | 800 | $1.35\times10^{-9}$ | $1.26\times10^{-9}$ | $1.44\times10^{-9}$ |
| **$0.625 < R < 1.18$** | 400 | $2.59\times10^{-9}$ | $1.24\times10^{-9}$ | $4.42\times10^{-9}$ |
| **(Larger particles)** | 800 | $2.84\times10^{-9}$ | $1.36\times10^{-9}$ | $4.86\times10^{-9}$ |

The medium particle range had the narrowest particle size distribution. It can be seen from Table 5.1. that there is a fairly significant change in diffusivities. However, most of the particles were likely at the upper range of the smaller particle range, and the lower range of the larger particle range based on visual observation (see bordered diffusivities in Table 5.1). Therefore subsequent calculations utilized an average $D_e$ value of $1.5\times10^{-9}$ $m^2/s$. The medium particle size range provided the narrowest diameter spread, having an average diameter of approximately 1.2 mm. A narrower particle size range produces $D_e$ data with a lower standard deviation. The variations in the effective diffusivity values were concluded to be a result of the assumed particle size used in the analysis for the other bin sizes.

The time for complete particle consumption was estimated using eqn. 2.10 and the average $D_e$ value for the medium particle size range. The results obtained were then compared with the time it would take if the pore diffusion–based calculated effective diffusivity value was used (see Table 2.2.).

To predict the $D_e$ values at plasma reactor conditions, i.e. 873 K, eqn. 2.13 was used. As mentioned in section 2.3, the ratio of $D_e$ to $D_{AB}$ is a constant (the linear correction term). Considering that the internal pore properties of the limestone particles were experimentally unknown, this constant represents these properties from the experimental data. Knowing the value of this constant and multiplying that with the $D_{AB}$ value at 873 K, gives the projected experimental effective diffusivity for the HCl-nitrogen mixture at plasma reactor conditions. From eqn. 2.13,

$$D_e = \frac{D_{AB}\phi_p\sigma_c}{\tau}, \text{ where } \frac{\phi_p\sigma_c}{\tau} = constant. \qquad (2.13)$$

Therefore knowing $D_e$ from the experiments and the calculated $D_{AB}$ at 408 K, the value of the constant can be approximated as $\frac{D_e}{D_{AB}} = \frac{1.5\times10^{-5}}{0.3106} = 4.82\times10^{-5}$

Recalculating $D_{AB}$ at $T$ = 873K and applying the determined linear scaling factor, yielded an effective diffusivity for HCl–Nitrogen at the elevated temperature of $5.61\times10^{-5}$ $cm^2/s$.

$$D_{e873K} = D_{AB873K} \times Constant = 1.165 \times 4.82 \times 10^{-5} = 5.61 \times 10^{-5} cm^2 / s$$

The experimental and theoretical results are summarized in Table 5.2. showing the time for complete particle reaction calculated using eqn. 2.10.

**Table 5.2.** Estimated Time for Complete Reaction of Limestone Particles with HCl.

| | $D_e$ ($m^2/s$) | Particle size range (mm) | Time (hrs) |
|---|---|---|---|
| **Experimental** $D_e$ **avg radius at 408K** | $1.5\times10^{-9}$ | $0.625 < R < 1.18$ | 505.95 |
| | | $0.584 < R < 0.625$ | 226.99 |
| | | $0.298 < R < 0.584$ | 120.67 |
| **Projected** $D_e$ **avg radius at 873K** | $5.61\times10^{-9}$ | $0.584 < R < 0.625$ | 60.51 |
| **Theoretical** $D_e$ **at 408K** | $3.13\times10^{-6}$ | $0.625 < R < 1.18$ | 0.23 |
| | | $0.584 < R < 0.625$ | 0.10 |
| | | $0.298 < R < 0.584$ | 0.05 |

The effective diffusivity values obtained can be seen to vary from the theoretically calculated value by several orders of magnitude. The 3-fold reduction in order of magnitude relates change from pore diffusion dominated mass transfer resistance to solid diffusion dominated resistance. The theoretical values on the order of $10^{-6}$ represent the diffusion taking place into the pores, and does not account for the increased resistance encountered as the HCl reacting front actually recedes into the limestone solid itself. Eqn. 2.13 showed that there is a linear correlation between the bulk diffusivity ($D_{AB}$) and effective diffusivity ($D_e$). The linear relationship from this equation is dependent on the pore properties of the particles, and as long as the pore properties of the particles do not change, this correlation is expected to remain the same.

As will be discussed in the following section, a similar linear scaling term was determined for HF adsorbing into the limestone particles. This suggests that there is a linear correction factor based on the internal properties of the solids. The effective gas diffusivities can be estimated at different temperatures from the product of the bulk diffusion of the gases and the linear correction factor. Therefore once the internal

properties of a solid particle are defined, the linear correction factor may be applied and a projection on the effective diffusivity of the gaseous substance into the solid at varying temperatures may be made.

Using the experimental effective diffusivity values and applying the shrinking core model, the rate at which the limestone solids would be converted under the experimental conditions is estimated and the results are shown in Fig 5.4.

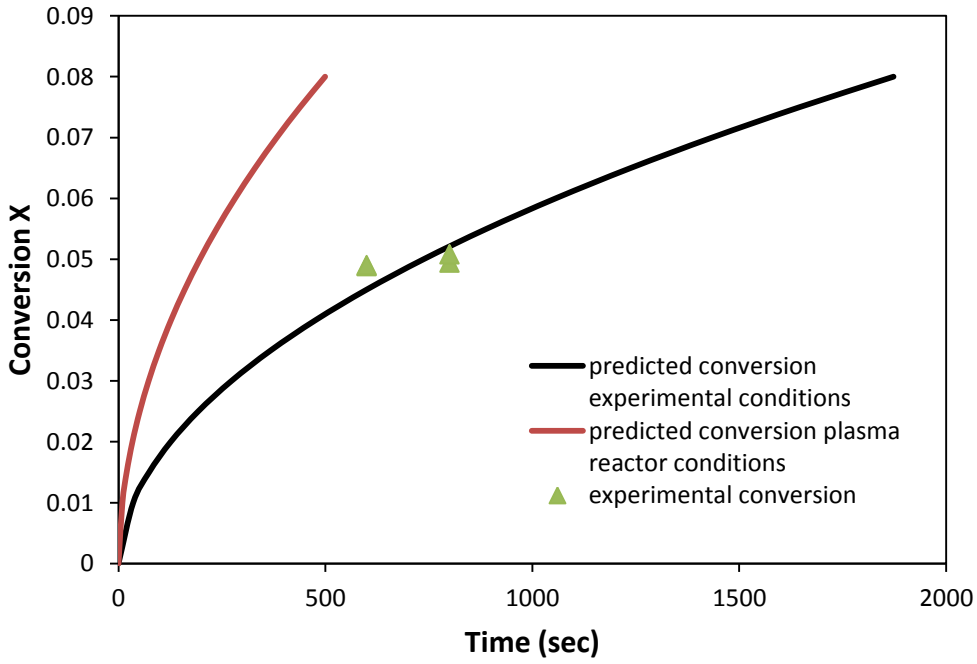


**Figure 5.4.** An estimation of the time it would take for the limestone particles with average particle radius 0.605 mm to be converted by the HCl gas at 408 K (experimental conditions) and 873 K (plasma reactor conditions).

*5.3.2.2. HF Gas as Adsorbate*

The HF experiments were carried out with continuous flow of 5% HF gas through the experimental system due to the reduced cylinder pressure available (below 140 psig). The same upstream pressure conditions were maintained for the HF experiments as for the HCl experiments. For the HF test, no blank run was conducted. The reactor was

packed with limestone particles using only the narrow particle size range $0.584 < R < 0.625$ mm with average radius of approximately 0.605 mm, and the duration of the gas runs were varied between 60 minutes and 210 minutes. As in the case of the HCl tests, the packed reactor was filled with limestone having particle size ranges obtained from the mesh screening. The results from a typical run using HF are shown in Fig 5.5.

The ideal gas equation was used to estimate the amount of HF gas that flowed through the entire system over the specific time frames. The amount of fluoride ion within the reacted solids was estimated to be between 13.6% and 19.9% of the amount of calcium present within the limestone (as described in Section 4.2. of Chapter 4). This was based on the assumption that 20% of the solid limestone was elemental calcium and therefore the fluoride ions that reacted would be present as calcium fluoride. The amount of HF gas that reacted for all the runs was also found to be between 7.8% and 16.2%. It was observed that for the shorter 60 minute run; the amount of HF gas that reacted with the limestone was greatest, followed by the 99 minute run, and finally the 209 minute run. This may be a result of the presence of a thicker product layer for the longer runs, which increases the time it takes for the gases to diffuse into the unreacted core resulting in slower reaction rates. Also, the percentage of gas that reacted for the 209 minute run was much smaller because the gas was run for a much longer time, though the reaction process was still the same as for the shorter time runs.

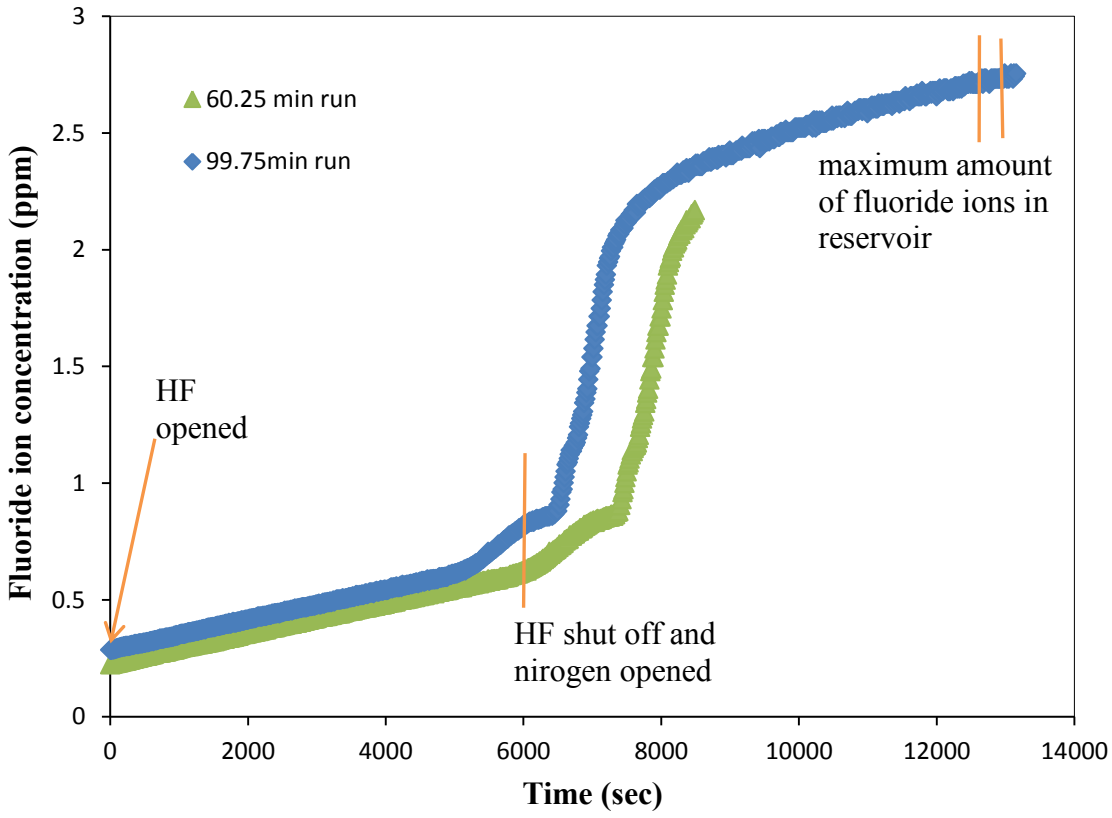


**Figure 5.5.** Typical breakthrough curves from the HF runs conducted at 60 and 99 minutes using the $0.584 < R < 0.625$ mm particle size range.

The amount of fluoride ion in the reservoir solution was found to be very small because calcium fluoride has very little solubility in water. Considering that most of the fluoride ions in the reservoir had been converted to calcium fluoride, the undissolved solids in the reservoir after the experiment accounted for the remaining fluoride ions that were not in solution. Supposing all the effluent HF flowing into the reservoir were converted into calcium fluoride, the change in undissolved solid mass seen in Table 5.3., gave a reasonable estimate of the expected results.

Furthermore, considering the amount of HF gas exiting the reactor, the amount of fluoride ion detected by the ISE and the change in mass of the undissolved solids within the reservoir before and after the experiment was run, the fluoride ions that entered the reactor but were undetected by the ISE were assumed to be present as calcium fluoride.

**Table 5.3.** Summary of the Amount of HF Adsorbed by Limestone in the Reactor and the Neutralization Reservoir

| Time for runs (minutes) | 99.75 | 99.25 | 60.25 | 209.20 |
|---|---|---|---|---|
| **Theoretical moles of HF fed based on flow rate and time (moles)** | 0.09009 | 0.08962 | 0.05445 | 0.18582 |
| **Fluoride ions adsorbed on limestone in reactor (moles)** | 0.01330 | 0.01452 | 0.00991 | 0.01456 |
| **HF exiting reactor into reservoir (moles)** | 0.07679 | 0.07510 | 0.04454 | 0.17126 |
| **Final measured Fluoride ion content in reservoir solution (moles)** | 0.00037 | 0.00017 | 0.00002 | 0.01243 |
| **Initial undissolved solids in reservoir (g)** | 8.2586 | 8.2512 | 8.2525 | Not measured |
| **Final undissolved solids in reservoir (g)** | 6.9998 | 6.9906 | 6.9919 | Not measured |
| **% of HF fed adsorbed by limestone** | 14.77 | 16.20 | 18.19 | 7.84 |
| **Initial mass of limestone particles in reactor** | 7.3226 | 7.3253 | 7.3267 | 7.3236 |
| **Final mass of limestone particles in reactor** | Not measured | Not measured | Not measured | 7.1297 |
| **% of limestone capacity in reactor used up** | 17.34 | 19.86 | 13.55 | 19.92 |

This was based on the assumption that if the undissolved solids were present as calcium carbonate, and the amount of HF gas that entered the reservoir completely reacted with the calcium carbonate, the resulting mass of the solids would be ~6.44 g. This value, though lower than the measured final solid mass (as seen in Table 5.3.) from the reservoir was close enough to the measured value to justify the lower fluoride ion concentration measured by the ISE. In addition, the relatively low solubility of calcium fluoride in water implies that the fluoride ions that reacted with the calcium ions present in the solution remained as calcium fluoride, thereby reducing the amount of fluoride ions in solution measured by the ISE.

The amount of fluoride ions adsorbed in the reactor as measured by the ISE was compared to the expected amount using the change in mass of the reactor solids during the experiment. To simplify the estimations, it was assumed that the initial mass of the solids was calcium carbonate and the final mass was a combination of calcium carbonate and calcium fluoride. To ascertain whether the estimated amounts of fluoride ions in the reactor was representative of what was expected,

Initial mass of $CaCO_3$ = 7.3236g  Final mass of solids = 7.1297g

Molar mass of $CaCO_3$ = 100.0869 $gmol^{-1}$  Molar mass of $CaF_2$ = 78.07 $gmol^{-1}$

Using $n = \frac{m}{M}$, where $n$ = moles of $CaCO_3$, $m$ = mass of $CaCO_3$ and $M$= molar mass of $CaCO_3$ = 100.0869 $gmol^{-1}$

$$n = \frac{7.3236}{100.0869} = 0.073236 mols$$

Initially, 0.073236 moles of $CaCO_3$ was present

At the end, $\frac{7.1297}{100.09y + 78.07(1-y)}$ moles of $CaCO_3$ and $CaF_2$ were present.

Where $y$ = mole fraction of $CaCO_3$ remaining after reaction with HF and

(1-$y$) = mole fraction of $CaF_2$formed after reaction

$$\frac{7.1297}{100.09y + 78.07(1-y)} = 0.073236$$

Therefore $22y = 19.35239$ and $y$ = 0.87965

(1-$y$)= 1 - 0.87965 = 0.12035

Therefore moles of $CaF_2$ = 0.12035×0.073236 = 0.00881 moles

From $CaF_2 \rightarrow Ca^{2+} + 2F^-$

n ( $F^-$) = 2× n ($CaF_2$) = 2×0.00881 = 0.017627 moles

Therefore 0.0176 moles of HF is expected to be adsorbed by the solids, based on the change in mass observed.

The initial amount of calcium carbonate present was calculated as 0.0732 moles and the final calculated amount of calcium fluoride was 0.0088 moles; this resulted in a final calculated fluoride content of 0.0176 moles. This amount is higher than the value measured by the ISE and this could be due to the fact that not all the solid is present as calcium carbonate. In addition, there could have been some moisture content within the solids which was lost as a result of heating at 408 K.

Assuming again that the solid limestone particles were spherical in shape, the shrinking core model was applied to the results obtained from the experimental runs to estimate the effective diffusivity ($D_e$) of the HF-nitrogen gas mixture into the limestone particles. Again, just as in the case of the HCl runs, the time values represent the time it takes for the HF gas to completely flow through the system. These were estimated from the breakthrough curves obtained. Just as in the case of the HCl runs, the $D_e$ values calculated for the HF runs based on the average particle radius were within the range of the lower and higher end radii. Thus in subsequent results, as seen in Table 5.4., the average effective diffusivity of the gas mixture was reported for the $0.584 < R < 0.625$ mm particle size range, with HF exposure times between 1 hour and 3.5 hours under the experimental conditions.

**Table 5.4.** Effective Diffusivity Estimation from the Experimental Data Using SCM (Particle Size Range $0.584 < R < 0.625$ mm at 408 K)

| **Time (sec)** | $\boldsymbol{D_{e\,avg}}$ **($m^2/s$)** |
|---|---|
| **3615** | $2.20\times10^{-9}$ |
| **5955** | $2.97\times10^{-9}$ |
| **6000** | $2.22\times10^{-9}$ |
| **12552** | $1.42\times10^{-9}$ |

To estimate the $D_e$ values at plasma reactor temperatures i.e. 873 K, it was assumed that the properties of the gas and the solids remained unchanged. In which case the value of the constant of proportionality from eqn. 2.13, calculated as the ratio of the

effective diffusivity to the bulk diffusivity for HF, would be $5.7\times10^{-5}$. The calculation procedure is described below and is similar to that used in the case of the HCl runs.

$$\text{Constant} = \frac{D_e}{D_{AB}} = \frac{2.2\times10^{-5}}{0.386} = 5.7\times10^{-5}$$

At plasma reactor temperatures, T = 873K, the projected effective diffusivity was thus determined as

$$D_{e873K} = D_{AB873K} \times Constant = 1.446\times5.7\times10^{-5} = 8.24\times10^{-5} cm^2/s$$

The time for complete particle consumption was estimated using equation 2.10, for the average $D_e$ values at the experimental conditions (see Table 5.4.) and the projected $D_e$ values at 873 K. The results obtained were then compared with the time it would take if the theoretical effective diffusivity value was used and these are summarized in Table 5.5.

From the results in Table 5.5., it can be seen that the effective diffusivity of the gas into the solids at the microwave plasma temperature is much higher and the time for complete particle reaction is drastically reduced. This indicates that temperature does affect the effective diffusivity of the gas into the solids which may be explained by the fact that the temperature of the gases was increased, and thus the movement of the gaseous molecules into the solids increased correspondingly.

**Table 5.5.** Estimated Time for Complete Reaction of Limestone Particles with HF.

| | **$D_e$ ($m^2/s$)** | **Time (hours)** |
|---|---|---|
| **Experimental $D_e$ avg at 408 K** | $2.20\times10^{-9}$ | 154.22 |
| **Projected $D_e$ avg at 873 K** | $8.24\text{x}10^{-9}$ | 41.20 |
| **Theoretical $D_e$ at 408 K** | $4.12\times10^{-6}$ | 0.08 |

Applying the shrinking core model and the obtained $D_e$ values, the conversion of the solids with respect to time was estimated and the results are shown in Fig 5.6.

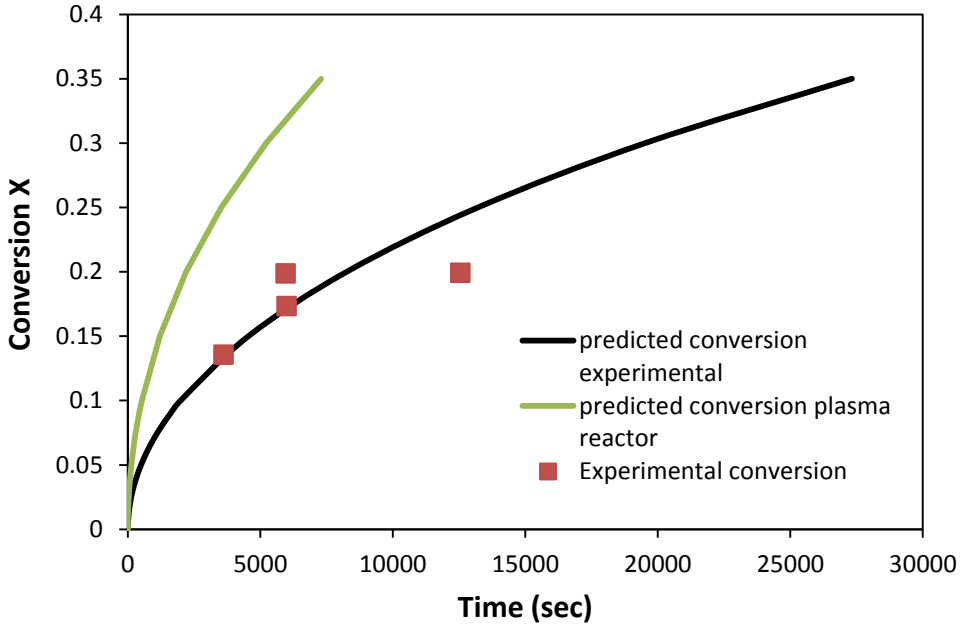


**Figure 5.6.** The estimated time at which the solid limestone particles with average particle radius 0.605 mm will be converted by the HF gases at 408 K (experimental conditions) and 873 K (plasma reactor conditions).

To explain why a linear correction term may be applicable to this study, the effective diffusivity and bulk diffusivity of the gases at 408 K and 873 K were compiled and their ratios determined. The results are seen in Table 5.6. Considering the minimal difference between the $D_e/D_{AB}$ ratios for HCl and HF, variations between the bulk and effective diffusivities were therefore assumed to be dependent on the internal properties of the solid particle which reduced the diffusivity of the gas into the solid.

**Table 5.6.** The Ratios of $D_e/D_{AB}$ at 408 and 873 K.

| **Temperature K** | **Gas** | $D_{AB}$ **(m²/s)** | $D_e$ **(m²/s)** | $D_e/D_{AB}$ **(%)** |
|---|---|---|---|---|
| **408** | HCl | $3.11\times10^{-5}$ | $1.50\times10^{-9}$ | 0.005 |
| | HF | $3.86\times10^{-5}$ | $2.20\times10^{-9}$ | 0.006 |
| **873** | HCl | $1.16\times10^{-4}$ | $5.560\times10^{-9}$ | 0.005 |
| | HF | $1.45\times10^{-4}$ | $8.20\times10^{-9}$ | 0.006 |

## 5.4. OTHER CONSIDERATIONS

It must be noted that during all the entire experimental runs, the gas flow rate was monitored via the pressure gauge to ensure that the flow rate remained approximately constant. Pressure drops observed were below 1 psig for the HCl and HF runs. Since the pressure was related to the gas flow rate, such a small pressure drop for the duration of the experiment makes it easier to estimate the flow rate of the gas and subsequently the amount of acidic gas that flowed through the system during the experiment.

## 5.5. PRACTICAL SYSTEM DESIGN

To estimate the minimum amount of solid limestone required to neutralize the acidic gases generated from the destruction of ~12,000 kg of waste refrigerants in the plasma reactor per month, the refrigerant difluoromethane ($CH_2F_2$) was used as an example to simplify the calculation.

At 873 K (600°C), the destruction of 12,000 kg of difluoromethane would generate ~0.0765 $m^3$ of HF/sec, or based on stoichiometric reaction with steam, 0.191 $m^3$/sec of gas for a six hour run occurring five working days in a week. Approximately 1,200 kg of calcium carbonate would be required to neutralize the generated HF gas based on the molar ratio for the reaction between calcium carbonate and HF. Assuming an HF concentration of 20% by volume, representing half of that which would be generated based on a stoichiometric reaction between $CH_2F_2$ and Water, approximately 15.6% of limestone particles would actually be utilized for the full 6 hour reaction time. This would result in an actual inventory requirement of 7400 kg. Using the Ergun equation and the parameters listed in Table 5.7., the required bed length and diameter needed to maintain a target pressure drop of 50,000 Pa was 12 m and 1.13 m, respectively.

**Table 5.7.** Parameters for Estimating the Bed Length in a ~1.1 m Diameter Reactor Vessel Filled with 7400 kg of Limestone, for a Gas Flow Rate of 0.0677 $m^3/s$.

| Parameter | For a set ΔP & reactor diameter, finding bed length | Units |
|---|---|---|
| **Bed length required** | 12.0 | m |
| **Mass of particles** | 7400 | kg |
| **Change in pressure ΔP** | 50000 | Pa |
| **Volumetric flow rate** | 0.191 | $m^3/s$ |
| **Bulk density** | 1515.55 | $kg/m^3$ |
| **Internal reactor diameter** | 1.13 | m |
| **Internal reactor cross Sectional area** | 1.0 | $m^2$ |
| **Dynamic viscosity of air $\mu$ at 600°C & 101.3 kPa** | 0.00004 | kg/m/s |
| **Density of air at 600°C & 101.3 kPa** | 0.4 | $kg/m^3$ |
| **Particle diameter** | 0.0012 | m |
| **Void fraction** | 0.41 | |
| **Superficial velocity** | 0.191 | m/s |
| **Interstitial velocity** | 0.467 | m/s |
| **Volume of vessel/bed needed for 0.4 void fraction** | 12 | $m^3$ |

## 5.6. SUMMARY

Comparing the experimentally obtained values from both the HCl and HF runs to the theoretically estimated values in Section 2.3., there is a difference between the effective diffusivity values and consequently in the time for complete particle conversion. Though these values differ, it must be noted that the theoretical effective diffusivity of HCl was lower than that of HF and the same trend was observed from the experimental $D_e$ values. The ratio of the theoretical effective diffusivities to the experimentally obtained values for HF and HCl was found to be fairly consistent, suggesting that there is a linear correction factor based on the internal properties of the solid, which relates the diffusivity of the gases into the solid particle with the bulk diffusion of the gases into a porous medium. As the gases diffuse into the solid particles, depending on the diffusion

mechanism in operation, it is expected that the diffusivity values would be less than what one would expect for a porous medium.

For illustrative purposes, previous studies on the effective diffusivity of nitrogen into solid materials at temperatures between 773 K and 1023 K yielded diffusivities on the order of $10^{-15}$ $m^2/s$.[78] This demonstrates the significantly lower diffusivity of gases into solid matrices.

Additionally, considering the efficiency of the slurry-based solution used to neutralize the unreacted effluent gases that entered the neutralization reservoirs, (see Chapter 4, Section 4.1), it is recommended that instead of a packed bed unit which does not sufficiently neutralize all the incoming gases and also has diffusivity limitations, a slurry-based unit be employed as a reasonable method to neutralize the acidic gases. The major challenge with the slurry-based solution is a reasonable estimation of the amount of acidic gases generated, which will in turn ensure a correct approximate estimation of the required amount of limestone and/or sodium bicarbonate needed to neutralize the inflowing acidic gases. In addition, a sensitive system for monitoring the concentration of the chloride and fluoride ions within the neutralization bath would need to be in place to ensure that the baths does not exceed its capacity for safe operations.

Under the experimental conditions and using the effective diffusivity values obtained under them, micron-sized particles would be required in order to obtain complete particle conversion times within seconds or minutes. This would require an entrained flow system and dust handling would have to be taken into consideration. The reactor set up for this study could not be used to investigate an entrained flow system and therefore this was not explored as part of this work.

# 6. CONCLUSIONS AND RECOMMENDATIONS

## 6.1. CONCLUSIONS

In summary, this work explores the feasibility of solid media adsorption for the neutralization of effluent acidic gases from a plasma reactor destroying waste refrigerants. The solid media considered for this purpose were cement powder and limestone.

Cement powder was found to be an unattractive solid adsorbent because it required large volumes to neutralize the acidic gases under the experimental conditions even as a powdery solid. It was found to adsorb only a fraction of the fed HF compared to limestone under the same conditions. In addition, it reduced the ability of other particles in the system to react with the HF gas. In contrast, limestone was found to be a relatively suitable alternative, though under the experimental conditions it did not neutralize the acids to the extent that was hoped for.

The results obtained showed that ~49% of the fed HCl and between 7.8% - 16.2% of the HF gases were adsorbed by seven grams of limestone for a flow rate of 0.4 L/min (STP) over 30 to 180 minutes. The total amount of limestone consumed by the HCl gas was found to be ~6.4% and between 13.6% and 19.9% for the HF gas.

The effective diffusivities of HCl and HF into the limestone particles under the experimental conditions ($T$ = 135°C) were $1.5\times10^{-9}$ and $2.2\times10^{-9}$ $m^2/s$, respectively and these values were used to estimate complete particle conversion times of 227 hours for HCl-limestone and 154 hours for HF-limestone. Furthermore, projected effective diffusivity values at plasma reactor temperatures (~873 K) reduced the particle consumption times to 61 hours for HCl and 41 hours for HF for the 1.2 mm diameter particles. These were obtained from effective diffusivity values of $5.61\text{x}10^{-9}$ $m^2/s$ and $8.24\text{x}10^{-9}$ $m^2/s$ for HCl and HF respectively.

Considering the long particle conversion times observed for the 1.2 mm particles, it may be possible to use smaller particles (micron–sized particles) to reduce these times into minutes or seconds. This would require entraining the particles in the gas flow for

the neutralization to occur. However, this was not tested as part of this study due to the nature of the reactor used.

The relative ratios of the theoretical effective diffusivities for HF and HCl to the experimentally obtained values suggested that there is a linear correction factor based on the internal solid properties of the solid particle, which related the bulk diffusion of the gases to the gas diffusivities within the solid particles. Therefore once the internal properties of a solid particle were defined, the linear correction factor was applied and a projection on the effective diffusivity of the gaseous substance into the solid was made. Variations between the bulk and effective diffusivities were therefore dependent on the internal properties of the solid particle and these reduced the diffusivity of the gas into the solid.

## 6.2. RECOMMENDATIONS

Based on the results presented in this work, the industry partner was advised to consider a liquid-based adsorption system to neutralize the acidic gases generated from the plasma reactor after waste refrigerant destruction. The potential to use solid-based systems may only be possible using smaller particle sizes, in which case the solids will have to be injected into the plasma reactor.

Should future work on the solid-based system proceed, it would need to be carried out at the plasma reactor conditions, and would require the injection of micron-sized solid particles to neutralize the acidic gases. The results from such a study would prove whether the complete particle reaction times would be on the order of seconds. A downstream liquid scrubbing unit would still be needed to meet emission requirements for these dangerous acidic gases.

Within the current experimental setup, future work could involve the study of temperature and effective diffusivity to see whether or not the predicted linear correction term applies for the extent of temperature increase applicable to the plasma reactor conditions.

## REFERENCES


1 Badr, O., Probert, S. D., & O'Callaghan, P. W. (1990). Chlorofluorocarbons and the environment: Scientific, economic, social and political issues. *Applied Energy, 37,* 4, 247-327.

2 Dickerman, J. C., Emmel, T. E., Harris, G. E., Hummel, K. E., & Radian Corp., Research Triangle Park, NC (USA). (1989). *Technologies for CFC (chlorofluorocarbons)/halon destruction. Final report, February-April 1989*. United States.

3 Murphy, A. B. (2003). Thermal plasma destruction of ozone-depleting substances: technologies and chemical equilibrium, chemical kinetic and fluid dynamic modelling. *High Temperature Material Processes, 7,* 4, 415-434.

4 Kryder, G., Springsteen, B., & Energy and Environmental Research Corp., Irvine, CA (United States). (1996). *Experimental investigation of PIC formation during CFC incineration. Final report, January-July 1995*. United States.

5 Ryan, J. V., Lee, C. W., Korn, S., & Acurex Environmental Corp., Research Triangle Park, NC (United States). (1993). *Organic emissions from pilot-scale incineration of CFCs*. United States.

6 Hall, R. E., Lee, C. W., Hassel, G. R., Ryan, J. V., & Energy and Environmental Research Corp., Irvine, CA (United States). (1991). *Experimental investigation of PIC formation in CFC incineration. Rept. for Jul-Sep 91*. United States.

7 Park, S.-W., Yoon, J.-H., & Lee, H. (1996). Destruction of CFC113 in Supercritical and Subcritical Water. *Korean Journal of Chemical Engineering, 13,* 6, 640-641.

8 Heberlein, J., & Murphy, A. B. (2008). Thermal plasma waste treatment. *Journal of Physics. D, Applied Physics, 41,* 5, 53001.

9 Heberlein, J. V. R. (1993). Thermal plasmas for the destruction of hazardous wastes. *Conference Proceedings Italian Physical Society, 37,* 59.

10 Sekiguchi, H., Honda, T., & Kanzawa, A. (1993). Thermal Plasma Decomposition of Chlorofluorocarbons. *Plasma Chemistry and Plasma Processing, 13,* 3, 463.

11 Yu, H., Kennedy, E. M., Adesina, A. A., & Dlugogorski, B. Z. (2006). A review of CFC and halon treatment technologies – The nature and role of catalysts. *Catalysis Surveys from Asia, 10,* 1, 40-54.

12 UNEP Technology and Economic Assessment Panel, UNEP Technology and Economic Assessment Panel Task Force on Collection, Recovery and Storage.& UNEP. Technology and Economic Assessment Panel Task Force on Destruction Technologies. (2002). *Montreal Protocol on Substances that Deplete the Ozone Layer: UNEP report of the Technology and Economic Assessment Panel, April 2002*. Namibia: UNEP.

13 Watanabe, T., & Shimbara, S. (2005). Halogenated Hydrocarbon Decomposition by Steam Thermal Plasmas. *Cheminform, 36,* 25.

14 Kettner, H. (1965). Removal of sulfur dioxide from flue gases. Review of various methods. *Bull. World Health Organ,* 421-9.

15 Sargent & Lundy LLC. (2002). *Graymont.* Retrieved July 11, 2013, from Graymont: http://www.graymont.ca/ technical/ Dry_ Flue_ Gas_ Desulfurization Technology Evaluation. pdf

16 Yasui, S., Shojo, T., Inoue, G., Koike, K., Takeuchi, A., & Iwasa, Y. (September 19, 2012). Gas-solid reaction properties of fluorine compounds and solid adsorbents for off-gas treatment from semiconductor facility. *International Journal of Chemical Engineering.*

17 Jena, P. R., De, S., & Basu, J. K. (2003). A generalized shrinking core model applied to batch adsorption. *Chemical Engineering Journal*, 95, 143-154.

18 Homma, S., Ogata, S., Koga, J., & Matsumoto, S. (2005). Gas–solid reaction model for a shrinking spherical particle with unreacted shrinking core. *Chemical Engineering Science*, 60, 18, 4971-4980.

19 Lee, K. T., & Koon, O. W. (2009). Modified shrinking unreacted-core model for the reaction between sulfur dioxide and coal fly ash/CaO/$CaSO_4$ sorbent. *Chemical Engineering Journal*, 146, 1, 57-62.

20 Xu, Z., Sun, X., & Khaleel, M. A. (2012). A generalized kinetic model for heterogeneous gas-solid reactions. *The Journal of Chemical Physics*, 137, 7.

21 Silva, H. S., Venturini, R. B., & Gonzalez, J. E. (2004). GAS-SOLID NON CATALYTIC REACTIONS: A MATHEMATICAL MODEL BASED ON HEAT TRANSFER ANALYSIS. Latin American Applied Research = Pesquisa Aplicada Latino Americana = Investigación Aplicada Latinoamericana, 34, 2, 111.

22 Sohn, H. Y., & Szekely, J. (1972). A structural model for gas-solid reactions with a moving boundary—III: A general dimensionless representation of the irreversible reaction between a porous solid and a reactant gas. *Chemical Engineering Science*, 27, 4, 763-778.

23 Peters, B., Dziugys, A., & Navakas, R. (2012). A shrinking model for combustion/gasification of char based on transport and reaction time scales. *Mechanika*, 18, 2, 177-185.

24 Hartmann, V. L. (2007). Gas–solid reaction modeling as applied to the fine desulfurization of gaseous feedstocks. *Chemical Engineering Journal*, 134, 190-194.

25 Liddell, K. N. C. (2005). Shrinking core models in hydrometallurgy: What students are not being told about the pseudo-steady approximation. *Hydrometallurgy*, 79, 62-68.

26 Yagi, S., & Kunii, D. (1955). Studies on combustion of carbon particles in flames and fluidized beds. *Symposium (international) on Combustion, 5,* 1, 231-244.

27 Levenspiel, O. (1999). Chemical reaction engineering. New York: Wiley.

28 Wen, C. Y. (1968). NON–CATALYTIC HETEROGENEOUS SOLID-FLUID REACTION MODELS. *Industrial & Engineering Chemistry*, 60, 9, 34-54.

29 Fogler, H. S. (2006). Elements of chemical reaction engineering. Upper Saddle River, NJ: Prentice Hall PTR.

30 Poling, B. E., Prausnitz, J. M., & O'Connell, J. P. (2001). The properties of gases and liquids. New York: McGraw-Hill.

31 Rigg, T. (1964), Kinetics of the reduction of ferrous chloride with hydrogen. *Can. J. Chem. Eng.*, 42: 247–253. doi: 10.1002/cjce.5450420603

32 Lu, W.-K., & Bitsianes, G. (1968). Chemical kinetics of gaseous reduction of hematite. *Canadian Metallurgical Quarterly*, 7, 1, 3-13.

33 Szekely, J., Evans, J. W., & Sohn, H. Y. (1976). Gas-solid reactions. New York: Academic Press.

34 Stephenson. (2008). *Agency for Toxic Substances and Disease Registry (ATSDR).* Retrieved July 10, 2012, from Centers for Disease control and prevention: http://www.atsdr.cdc.gov/toxprofiles/tp11-c5.pdf

35 J. Aigueperse, P. M. (2005). Fluorine compounds, Inorganic. In *Ullman's Encyclopedia of Industrial Chemistry* (pp. 397-441). Weinheim: Wiley-VCH.

36 *Chemicalland21*. (n.d.). Retrieved July 11, 2012, from http://www.chemicalland21.com/industrialchem/inorganic/ALUMINUM FLUORIDE.htm

37 H.F.J. Denzinger, H. K. (1979). Fluorine recovery in the fertilizer industry - a review. *Phosphorus and Potassium* , 33-39.

38 IHS. (n.d.). Retrieved July 11, 2012, from IHS Chemical: http://www.ihs.com/products/chemical/planning/ceh/fluorspar-and-inorganic-fluorine.aspx

39 ALCOA. (n.d.). *AWAM North America*. Retrieved July 11, 2012, from ALCOA Aluminum fluoride: http://www.alcoa.com/alumina_minerals/north_america/en/products/ product3.asp

40 ALCOA. (n.d.). Retrieved July 11, 2012, from ALCOA Aluminum Fluoride MSDS: http://www.alcoa.com/global/en/environment/msdsview.asp?LoadMSDS=203541

41 Sigma-Aldrich Co, LLC. (n.d.). Retrieved July 11, 2012, from Sigma Aldrich: http://www.sigmaaldrich.com/MSDS/MSDS/DisplayMSDSPage.do?country=CA&language=en&productNumber=563919&brand=ALDRICH&PageToGoToURL=http%3A%2F%2Fwww.sigmaaldrich.com%2Fcatalog%2Fproduct%2Faldrich%2F563919%3Flang%3Den

42 (2012). Retrieved July 18, 2012, from Platts: http://www.platts.com/AluminaPAXBenchmark?WT.srch=1

43 Reynolds, M. (2010). *Aluminium today*. Retrieved May 17, 2013, from Aluminium today: http:// www.aluminiumtoday.com/ contentimages/features/PrimaryFluoride. pdf

44 (1999-2000). Retrieved July 18, 2012, from Alibaba.com: http://www.alibaba.com/showroom/price-for-aluminum-chloride.html

45 Miller, M. M. (2004). Retrieved May 17, 2013, from US Geological Survey: http://minerals.usgs.gov/minerals/pubs/commodity/fluorspar/fluormyb04.pdf

46 (n.d.). Retrieved July 11, 2012, from mineral information institute: http://www.mii.org/Minerals/photofluor.html

47 Rothrock, H. E. (n.d.). Fluorspar. *NEW MEXICO GEOLOGICAL SOCIETY—TWENTY-FIRST FIELD CONFERENCE* , 123-125.

48 Solvay Chemicals. (n.d.). Retrieved July 11, 2012, from Solvay chemicals: http://www.solvaychemicals.us/SiteCollectionDocuments/sds/P19190-USA.pdf

49 (n.d.). Retrieved July 11, 2012, from ICIS.com: http://www.icis.com/Articles/2004/03/12/564646/chemical-prices-for-week-ending-march-12-2004.html

50 (1999-2012). Retrieved July 18, 2012, from Alibaba.com: http://www.alibaba.com/ showroom/ calcium-carbonate-price.html

51 NoahTechnologies Corporation. (n.d.). Retrieved July 11, 2012, from Noah Technologies Corporation: http://www .noahtech.com/ frameset.asp?id = catalogsearch

52 (1999-2012). Retrieved July 18, 2012, from Alibaba.com: http://www.alibaba.com/trade/search?SearchText=calcium+fluoride+price&IndexArea=product_en&fsb=y

53 (1999-2012). Retrieved July 18, 2012, from Alibaba.com: http://www.alibaba.com/trade/search?SearchText=price+for+calcium+chloride&IndexArea=product_en&fsb=y

54 Solvay chemicals. (n.d.). Retrieved July 11, 2012, from Solvay Chemicals: http://www.solvaychemicals.us/SiteCollectionDocuments/sds/P31-USA.pdf

55 EPA. (n.d.). Retrieved July 11, 2012, from EPA R.E.D. : http://www.epa.gov/oppsrrd1/REDs/sodium-fluoride-red.pdf

56 (n.d.). Retrieved July 11, 2012, from Livestrong.com: http://www.livestrong.com/article/344745-common-uses-of-sodium-fluoride/

57 Pradyot Patnaik, P. (2003). *Handbook of Inorganic Chemicals.* United States of America: McGraw-Hill.

58 (1999-2012). Retrieved July 18, 2012, from Alibaba.com: http://www.alibaba.com/trade/search?SearchText=sodium+hydroxide+price&IndexArea=product_en&fsb=y

59 (1999-2012). Retrieved July 18, 2012, from Alibaba.com: http://www.alibaba.com/trade/search?SearchText=sodium+carbonate+price&IndexArea=product_en&fsb=y

60 (1999-2012). Retrieved July 18, 2012, from Alibaba.com: http://www.alibaba.com/trade/search?SearchText=sodium+fluoride+price&IndexArea=product_en&fsb=y

61 (n.d.). Retrieved July 11, 2012, from Light machinery: http://www.lumonics.com/Materials/MgFl.pdf

62 (1999-2012). Retrieved July 18, 2012, from Alibaba.com: http://www.alibaba.com/trade/search?SearchText=magnesium+carbonate+price&IndexArea=product_en&fsb=y

63 (1999-2012). Retrieved July 18, 2012, from Alibaba.com: http://www.alibaba.com/trade/search?SearchText=magnesium+fluoride+price&IndexArea=product_en&fsb=y

64 Chemical book. (2008). Retrieved May 17, 2013, from Chemical book: http://www.chemicalbook.com/ProductChemicalPropertiesCB5250422_EN.htm

65 (1999-2013). Retrieved August 5, 2013, from Alibaba.com: http://www.alibaba.com/trade/search?fsb=y&IndexArea=product_en&CatId=&SearchText=iron

66 (2013). Retrieved August 5, 2013, from VWR International LLC: https://us.vwr.com/store/catalog/product.jsp?product_id=7485241

67 (1999-2013). Retrieved August 5, 2013, from Alibaba.com: http://www.alibaba.com/trade/search?fsb=y&IndexArea=product_en&CatId=&SearchText=iron+ii+chloride

68 Cameo Chemicals. (n.d.). Retrieved May 17, 2013, from Cameo Chemicals: http://cameochemicals.noaa.gov/chemical/3468

69 Lafarge. (2012). *Lafarge.* Retrieved July 11, 2012, from Lafarge: http://www.lafarge-na.com/MSDS_North_America_English_-_Portland_Cement.pdf?xtmc=portlandcementmsds&xtcr=1

70 (2010). Retrieved July 11, 2012, from Connexions: http://cnx.org/content/m16445/latest/

71 Anna Emmanuelson, Staffan Hansen, Erik Viggh. (2003). A comparative study of ordinary and mineralised Portland cement clinker from two different production units. Part I: Compostion and Hydration of Clinkers. *Cement and concrete research* , 1613-1621.

72 American Society of Concrete Contractors (n.d.). Retrieved August 3, 2013, from American Society of Concrete Contractors: http://www.ascconline.org/PositionStatements/PS31CalciumChlorideWebSC.pdf

73 Whiting, D. A., Taylor, P. C., & Nagi, M. A. (2002). Chloride Limits in Reinforced Concrete. Illinois: Portland Cement Association.

74 (1999-2012). Retrieved July 19, 2012, from Alibaba.com: http://www.alibaba.com/showroom/fly-ash-price.html

75 Aerosmith, I. (n.d.). Retrieved September 25, 2012, from http://www.idealvalve.com/pdf/Flow-Calculation-for-Gases.pdf

76 Kurita, C. H. (1988). Retrieved September 25, 2012, from http://lss.fnal.gov/archive/d0-en/fermilab-d0-en-173.pdf

77 Szekely, J., Evans, J. W., & Sohn, H. Y. (1976). Gas-solid reactions. New York: Academic Press.

78 Alpass, C. R., Murphy, J. D., Wilshaw, P. R., Jain, A., & High Purity Silicon 10 - 214th ECS Meeting. (2008). Measurements of dislocation locking by near-surface ion-implanted nitrogen in Czochralskisilicon. *Ecs Transactions, 16,* 6, 249-259.

# APPENDICES

## A1. ESTIMATING THEORETICAL EFFECTIVE DIFFUSIVITIES ($D_e$) FOR THE ACIDIC GASES INTO LIMESTONE PARTICLES AT 408 K (135°C).

***For the HCl – Nitrogen Mixture***

T = 408K

$$\frac{\varepsilon_{AB}}{k} = (344.7 \times 71.4)^{1/2} = 156.881$$

$$T^* = \frac{kT}{\varepsilon_{AB}} = \frac{1}{156.881} \times 408 = 2.6007$$

$$\Omega_D = \frac{1.06036}{(2.6007)^{0.15610}} + \frac{0.19300}{\exp(0.47635 \times 2.6007)} + \frac{1.03587}{\exp(1.52996 \times 2.6007)} + \frac{1.76474}{\exp(3.89411 \times 2.6007)} = 0.98$$

$$\delta_A = \frac{1.94 \times 10^3 \times 1.1^2}{30.28 \times 188.15} = 0.412 \qquad \delta_B = \frac{1.94 \times 10^3 \times 0.0^2}{34.84 \times 77.35} = 0.0$$

$$\delta_{AB} = (0.412 \times 0.0)^{1/2} = 0$$

$$\Omega_D^* = 0.98 + \frac{0.19 \times 0.0^2}{2.6007} = 0.98$$

$$\sigma_{AB} = (3.339 \times 3.798)^{1/2} = 3.5611$$

$$M_{AB} = 2\left(\frac{1}{36.461} + \frac{1}{28.014}\right)^{-1} = 31.68$$

P = 1 bar

Therefore diffusion coefficient $D_{AB} = \frac{0.00266(408)^{3/2}}{1 \times 31.68^{1/2} \times 3.5611^2 \times 0.98} = 0.3107 cm^2/s$

And the effective diffusivity $D_e = \frac{0.3134 \times 0.4 \times 0.8}{3.0} = 0.0313 cm^2/s$

***For the HF – Nitrogen Mixture***

T = 408K

$$\frac{\varepsilon_{AB}}{k} = (330 \times 71.4)^{1/2} = 153.499$$

$$T^* = \frac{kT}{\varepsilon_{AB}} = \frac{1}{153.499} \times 408 = 2.65799$$

$$\Omega_D = \frac{1.06036}{(2.6579)^{0.15610}} + \frac{0.19300}{\exp(0.47635 \times 2.6579)} + \frac{1.03587}{\exp(1.52996 \times 2.6579)} + \frac{1.76474}{\exp(3.89411 \times 2.6579)} = 0.9824$$

$$\delta_A = \frac{1.94 \times 10^3 \times 1.8^2}{20.69 \times 292.68} = 1.038 \quad \delta_B = \frac{1.94 \times 10^3 \times 0.0^2}{34.84 \times 77.35} = 0.0$$

$$\delta_{AB} = (1.038 \times 0.0)^{1/2} = 0$$

$$\Omega_D^* = 0.9824 + \frac{0.19 \times 0.0^2}{2.6579} = 0.9824$$

$$\sigma_{AB} = (3.148 \times 3.798)^{1/2} = 3.4578$$

$$M_{AB} = 2\left(\frac{1}{20.006} + \frac{1}{28.014}\right)^{-1} = 23.342$$

P = 1 bar

Therefore diffusion coefficient $D_{AB} = \frac{0.00266(408)^{3/2}}{1 \times 23.342^{1/2} \times 3.4578^2 \times 0.9824} = 0.3863 cm^2/s$

And the effective diffusivity $D_e = \frac{0.3863 \times 0.4 \times 0.8}{3.0} = 0.0412 cm^2/s$

## A2. CALIBRATION DATA FOR GAS FLOW RATE USING THE ROTAMETER

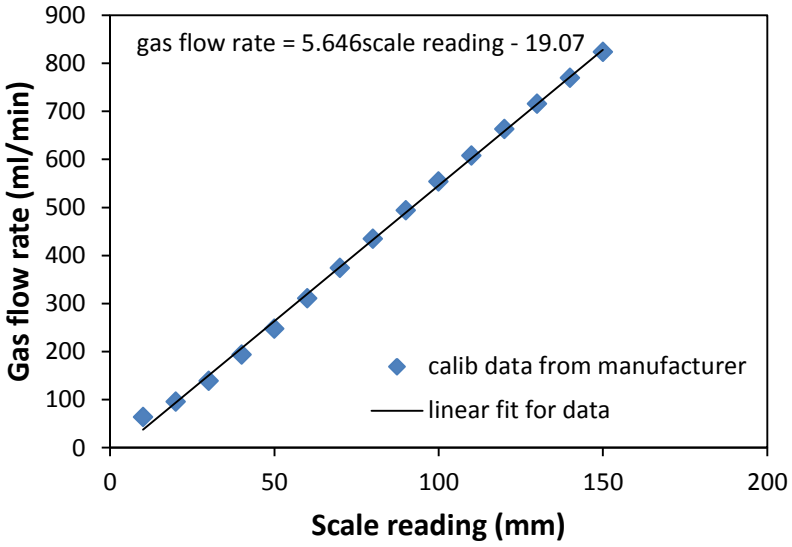


**Figure A2.1.** Calibration chart for Omega FL-3802ST gas flow meter using nitrogen gas. Data obtained from provided manufacturer's data.

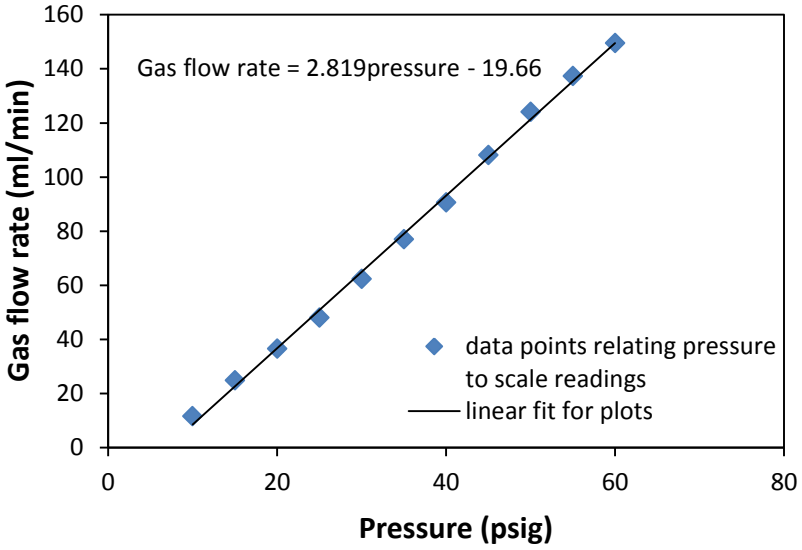


**Figure A2.2.** Relationship between upstream pressure and rotameter reading for nitrogen flowing through CFO under atmospheric downstream conditions as obtained from experiment.

Combining Figs A2.1. and A2.2. resulted in Fig 4.2. shown in Chapter 4.

## A3. OPERATING THE ELECTRIC FURNACE

Put on personal protective equipments (lab coat, gloves and safety glasses).

Put on hood fans.

Close the furnace door and lock it.

Plug the control box plug into the power source and watch the lights and indicators on the controller come on.

Insert furnace thermocouples into the furnace via the holes in the front of the furnace, to monitor the temperature of the furnace.

Plug the furnace plug into the power source.

Set the furnace temperature (See Fig A3.1) by using the up (6) and down (7) arrow keys on the control box to the desired temperature. Watch the bottom number (4) on the control for the set furnace temperature.

Press and hold the refresh button on the controller until the last number of (3) has a dot after it and is blinking. Then release the button.

Watch (3) as the actual temperature rises to the set temperature on (4).

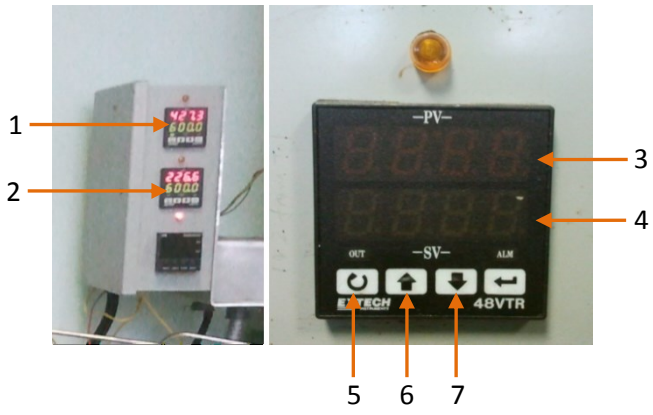


**Figure A3.1.** Furnace temperature controls

KEY:

1. Top furnace controller
2. Bottom furnace controller
3. Temperature of furnace as indicated by thermocouples
4. Required temperature of furnace
5. Refresh button for auto-tuning
6. Up arrow for temperature increases
7. Down arrow for temperature decreases

Wait for 20 minutes for the furnace temperature to stabilize at the set temperature.

Leave the furnace on for the intended process, most likely an hour or two.

After the process, unplug the furnace plug from the power source.

Leave the furnace thermocouples in the furnace to indicate the temperature of the furnace on (3).

Unplug the control box plug and leave the furnace overnight to cool.

- To know if the furnace is cooled, plug in the control box plug and read the actual furnace temperature (3) from the controller via the inserted thermocouples.

If furnace temperature is room temperature or close to room temperature, it is safe to open.

## A4. ESTIMATING THE CONCENTRATION OF SODIUM BICARBONATE FOR THE NEUTRALIZATION RESERVOIRS

To estimate the amount of sodium bicarbonate needed for complete neutralization of the incoming gases, the amount of HCl gas flowing into the reservoir was estimated using the ideal gas equation and an estimated run time of 60 minutes assuming there were no solid limestone particles in the reactor. Also, a flow rate of approximately 426 mL/min which was equivalent to a pressure of 35 psig was used in the estimation of the volume of HCl flowing into the reservoir.

P = 1 atm  R = 0.0821 $LatmK^{-1}mol^{-1}$  T = 20°C = 293 K

V = 5% HCl = 0.05×426mL/min = 21.3 mL/min

Therefore over 60 minutes, approximately 1278 mL of HCl would have flown into the reservoir.

From $PV = nRT$, $n = \frac{PV}{RT} = \frac{1atm \times 1.278L}{0.0821LatmK^{-1}mol^{-1} \times 293K} = 0.0531mols$

From the balanced reaction equation, $NaHCO_3 + HCl \longrightarrow NaCl + H_2O + CO_2$

$\frac{n(HCl)}{n(NaHCO_3)} = \frac{1}{1}$; Therefore $n(HCl) = n(NaHCO_3) = 0.0531moles$

From $n = \frac{m}{M}$, where $n$ = moles of $NaHCO_3$, $m$ = mass of $NaHCO_3$ and $M$= molar mass of $NaHCO_3$ = 84.007 $gmol^{-1}$

$$\Rightarrow m = n \times M = 0.0531mols \times 84.007gmol^{-1} = 4.4631g$$

This implies that for a 5% v/v HCl concentration with a flow rate of 426mL/min for 60 minutes, in the absence of any solid in the reactor, 4.4631 g of sodium bicarbonate is required to completely neutralize the incoming acidic gas. To be cautious, since the experiments may be run longer than 60 minutes and also, to avoid exceeding the capacity of the neutralization reservoir, the estimated mass was doubled. After weighing the actual

solids using a Sartorius CP 124S mass balance with ±0.0001 g accuracy, a mass of approximately 7.8442 g was used in all the runs.

The concentration of the sodium bicarbonate solution was estimated as shown below.

$n = \frac{m}{M} = \frac{7.8442g}{84.007gmol^{-1}} = 0.09338mols$ , therefore in a 2.5 L volume of solution

Concentration of $NaHCO_3$,

$$C = {}^{n}\!/_{V} = {}^{0.09338mols}\!/_{2.5L} = 0.037352molL^{-1} = 0.0374M$$

For the HF runs, the concentration of the gas was again 5% v/v and it was run under the same conditions as the HCl experiments. Therefore, the concentration of sodium bicarbonate in the neutralization reservoirs was the same as that for the HCl runs, i.e. 0.0374 M in a 2.5 L volume. However, in addition to the sodium bicarbonate, limestone was also dissolved in the solution. This was done because sodium fluoride, which would be formed from the reaction between sodium bicarbonate and hydrofluoric acid (HF), is a relatively unstable salt when compared to calcium fluoride, though HF reacts rapidly with sodium ions than it does with calcium ions. Considering the hazardous nature of sodium fluoride, it was decided to add limestone to provide a calcium source to react with the fluoride ions after they have reacted with the sodium ions, leading to a much stable salt formation which can be relatively easier to handle.

The concentration of limestone (Calcium carbonate, $CaCO_3$) used was the same as that of sodium bicarbonate (0.0374 M), based on the assumption that all the sodium fluoride would end up converted to calcium fluoride. The mass of $CaCO_3$ that was required to prepare a 2.5 L volume of 0.0374 M limestone solution was estimated as shown below.

From $C = {}^{n}\!/_{V}$, $n = C \times V = 0.0374molL^{-1} \times 2.5L = 0.0935mols$ of $CaCO_3$

From $n = \frac{m}{M}$, where $n$ = moles of $CaCO_3$, $m$ = mass of $CaCO_3$ and $M$= molar mass of $CaCO_3$ = 100.0869 $gmol^{-1}$

$$\Rightarrow m = n \times M = 0.0935 mols \times 100.0869 g mol^{-1} = 9.3581 g$$

Therefore for a 5% v/v HF gas with a 426 mL/min flow rate for 60 minutes, in the absence of any solid material in the reactor, approximately 9.3581 g of limestone would be needed to completely react with the unstable fluoride ions present as sodium fluoride. It must be noted however, that especially for the HF experiments exceeding two hours, the sodium bicarbonate and calcium carbonate amounts were tripled for safety.

Furthermore, for both the HCl and HF runs, the chloride and fluoride ion measurements by the ISE meter were not allowed to exceed the 200 ppm mark.

## A5. CALIBRATING THE ION SELECTIVE ELECTRODE

A chloride ion selective BNC probe (Cole Parmer, K-27502-07) and fluoride BNC probe (Cole Parmer, K-27502-19) were monitored by a Thermo Scientific Orion Dual Star ™ pH/ISE meter with model number E05289 during the HCl and HF runs respectively.

The provided Reference fill solutions for the probes were 10% potassium nitrate ($KNO_3$) and 4 M potassium chloride (KCl) for the chloride and fluoride probes respectively. The probes were calibrated using the accompanying sodium chloride and sodium fluoride calibration solutions provided by the manufacturer. There was also a stainless steel Thermo Scientific ATC probe with an 8 pin MD detector having a relative accuracy of ± 1°C connected to the pH/ISE meter to measure the temperature of the solution.

To calibrate the meter for both HCl and HF runs, the maximum amount of chloride and fluoride ions that would enter the first neutralization reservoir and therefore be measured by the inserted probe was estimated to be approximately 510 ppm. 100 ml standard solutions of 1000, 500, 400, 300, 150 and 50 ppm sodium chloride (NaCl) were prepared from the provided 1000 ppm standard and used to calibrate the meter for Chloride ion measurements before the HCl runs were conducted.

After the calibrated probe was used to measure chloride ions in a sample of the 0.0395 M ± 0.0029 M sodium bicarbonate solution used in the neutralization reservoir, it was noted that the measurement recorded by the meter was much higher than the expected concentration of chloride ions that were put into the solution. This was attributed to the presence of other ions ($Na^+$, $CO_3^{2-}$) in the solution, which most likely contributed to the oxidation-reduction potential of the solution and in effect was measured by the meter. To correct this anomaly so that the measurements recorded reflected the actual amount of chloride ions present, a corrected calibration curve was prepared using the sodium bicarbonate solution and known volumes of chloride solution. This new curve was used to correct the measured chloride ion content within the first neutralization bath. For the chloride ion amounts within the reacted solids, the normal calibration curve was used because of there was no sodium bicarbonate in the base solution. The oxidation-reduction potential (ORP) measurements from the meter in mV were related to the actual

concentration of chloride ions added to the solution and this new calibration curve, shown in Fig. A5.1, was used in subsequent experiments.

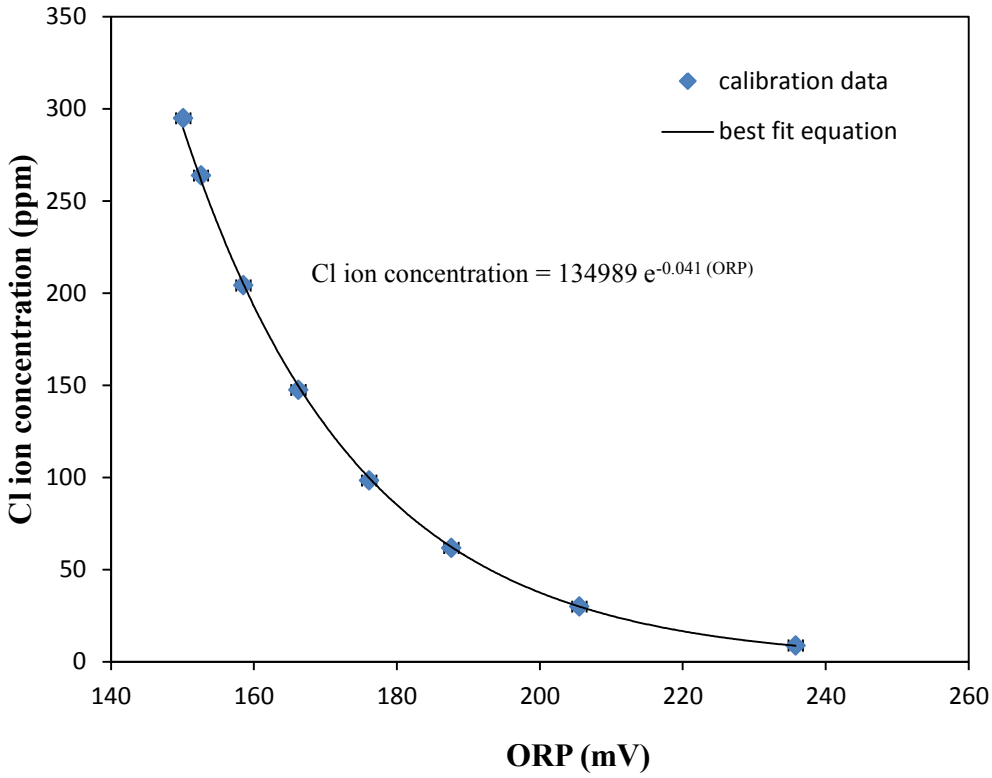


**Figure A5.1.** Calibration curve for the chloride ion selective probe used to measure the chloride ion concentration in a 0.0395 M ± 0.0029 M sodium bicarbonate solution in the first neutralization reservoir. Error bars have a fixed value of ±1 mV.

To calibrate the fluoride probe, 100 ml standard solutions of 1000, 500, 250, 125, 50 and 5 ppm sodium fluoride (NaF) were prepared from the provided 1000 ppm standard. The 125 ppm solution was later removed because its ORP measurements were very close to that of the 250 ppm solution and the meter could therefore not record its measurements for use in the calibration curve. A potential error that was mentioned in the instruction manual. Furthermore, because of the prior changes made to the chloride calibration curve, similar checks by adding known amounts of sodium fluoride to the sodium bicarbonate - limestone solution, and measuring the fluoride concentration were made. Again, the measured fluoride concentrations were above the calculated amounts of

the ions added. Therefore a modified calibration curve, using the ORP measurements and the calculated fluoride ion concentrations was made (see Fig A5.2) and this was used to correct the fluoride ion measurements in the first neutralization reservoir for the HF runs. For the fluoride ion measurements within the solids, the actual calibration curve (obtained using deionized water and standard) was used because of the absence of the sodium bicarbonate and limestone in the base solution. The negative ORP values obtained indicate that the solution has strong reducing properties. This reducing ability was to increase as the fluoride ion concentration increased and therefore it can be said that the reducing nature of the fluoride ions resulted in the negative ORP measurements made by the ISE meter.

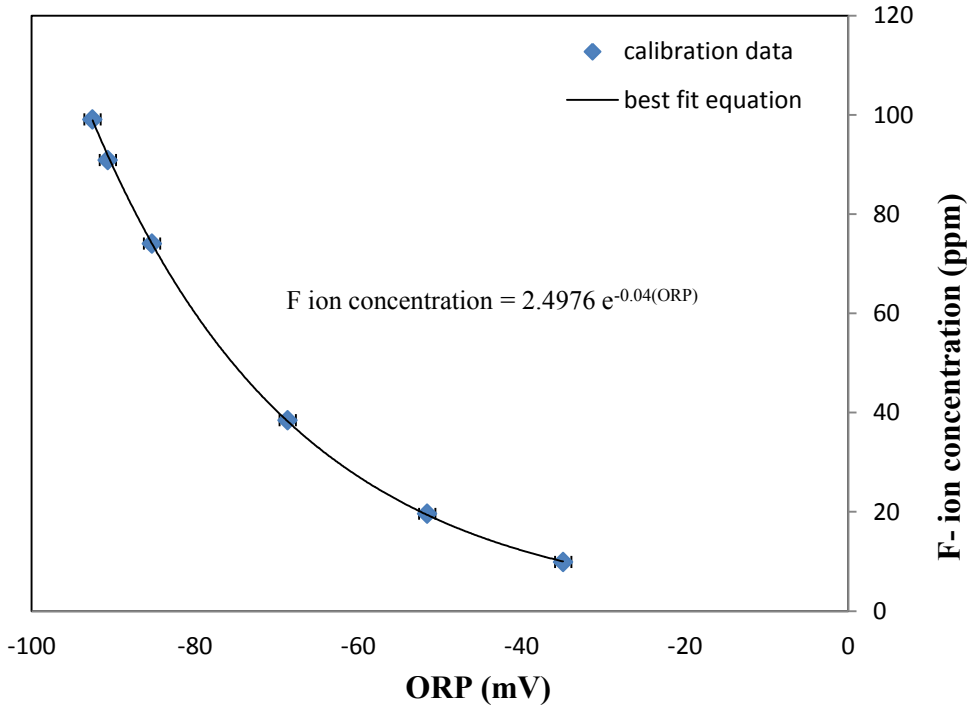


**Figure A5.2.** Calibration curve for the fluoride ion selective probe used to measure the fluoride ion concentration in a 0.0614 M ± 0.0013 M sodium bicarbonate - 0.0373 M ± 0.0001 M limestone solution in the first neutralization reservoir. Error bars have a fixed value of ±1 mV

## A6. SETTING UP THE ISE METER FOR TIMED READINGS

Plug and press the POWER button to put on the meter.

Press the F3 button and select READ TYPE from the list of options.

Use the down arrow and select the ‘AT TIME INTERVAL’ option.

Enter the time interval at which you want measurements to be taken. Note that the time format is Hours:Minutes:Seconds.

Press the button under the ACCEPT tab and then BACK.

The meter is now ready to measure at the set time interval.

## A7. ESTIMATING THE EFFECTIVE DIFFUSIVITIES ($D_e$) AT 873 K (600°C)

$$D_e = \frac{D_{AB}\phi_p\sigma_c}{\tau}, \text{ where } \frac{\phi_p\sigma_c}{\tau} = constant.$$

Therefore knowing $D_e$ from the experiments and $D_{AB}$, the value of the constant can be approximated as $\frac{D_e}{D_{AB}} = constant$

***For the HCl – Nitrogen Mixture***

$$\frac{D_e}{D_{AB}} = \frac{1.5\times10^{-5}}{0.3106} = 4.82\times10^{-5}$$

T = 873 K

$$\frac{\varepsilon_{AB}}{k} = \left(344.7\times71.4\right)^{1/2} = 156.881$$

$$T^* = \frac{kT}{\varepsilon_{AB}} = \frac{1}{156.881}\times873 = 5.5647$$

$$\Omega_D = \frac{1.06036}{(5.5647)^{0.15610}} + \frac{0.19300}{\exp\left(0.47635\times5.5647\right)} + \frac{1.03587}{\exp\left(1.52996\times5.5647\right)} + \frac{1.76474}{\exp\left(3.89411\times5.5647\right)} = 0.825$$

$$\delta_A = \frac{1.94\times10^3\times1.1^2}{30.28\times188.15} = 0.412 \quad \delta_B = \frac{1.94\times10^3\times0.0^2}{34.84\times77.35} = 0.0$$

$$\delta_{AB} = \left(0.412\times0.0\right)^{1/2} = 0$$

$$\Omega_D^* = 0.825 + \frac{0.19\times0.0^2}{5.5647} = 0.825$$

$$\sigma_{AB} = \left(3.339\times3.798\right)^{1/2} = 3.5611$$

$$M_{AB} = 2\left(\frac{1}{36.461} + \frac{1}{28.014}\right)^{-1} = 31.68$$

P = 1 bar

Therefore diffusion coefficient $D_{AB} = \frac{0.00266(873)^{3/2}}{1 \times 31.68^{1/2} \times 3.5611^2 \times 0.825} = 1.165 cm^2/s$

$D_{e873K} = D_{AB} \times Constant = 1.165 \times 4.82 \times 10^{-5} = 5.61 \times 10^{-5} cm^2/s$

***For the HF – Nitrogen Mixture***

$\frac{D_e}{D_{AB}} = \frac{2.2 \times 10^{-5}}{0.386} = 5.7 \times 10^{-5}$

T = 873 K

$\frac{\varepsilon_{AB}}{k} = (330 \times 71.4)^{1/2} = 153.499$

$T^* = \frac{kT}{\varepsilon_{AB}} = \frac{1}{153.499} \times 873 = 5.687$

$\Omega_D = \frac{1.06036}{(5.687)^{0.15610}} + \frac{0.19300}{\exp(0.47635 \times 5.687)} + \frac{1.03587}{\exp(1.52996 \times 5.687)} + \frac{1.76474}{\exp(3.89411 \times 5.687)} = 0.821$

$\delta_A = \frac{1.94 \times 10^3 \times 1.8^2}{20.69 \times 292.68} = 1.038$ $\delta_B = \frac{1.94 \times 10^3 \times 0.0^2}{34.84 \times 77.35} = 0.0$

$\delta_{AB} = (1.038 \times 0.0)^{1/2} = 0$

$\Omega_D^* = 0.821 + \frac{0.19 \times 0.0^2}{5.687} = 0.821$

$\sigma_{AB} = (3.148 \times 3.798)^{1/2} = 3.4578$

$M_{AB} = 2\left(\frac{1}{20.006} + \frac{1}{28.014}\right)^{-1} = 23.342$

P = 1 bar

Therefore diffusion coefficient $D_{AB} = \frac{0.00266(873)^{3/2}}{1 \times 23.342^{1/2} \times 3.4578^2 \times 0.821} = 1.446 cm^2/s$

$D_{e873K} = D_{AB} \times Constant = 1.446 \times 5.7 \times 10^{-5} = 8.24 \times 10^{-5} cm^2/s$